

Summer 2024

Refinement of a Regional Storm Surge Mesh for High-Resolution Topographic Representation of Volusia County

Morgan Harbin

Embry-Riddle Aeronautical University, harbinm@my.erau.edu

Follow this and additional works at: <https://commons.erau.edu/edt>



Part of the [Civil Engineering Commons](#), [Environmental Engineering Commons](#), and the [Hydraulic Engineering Commons](#)

Scholarly Commons Citation

Harbin, Morgan, "Refinement of a Regional Storm Surge Mesh for High-Resolution Topographic Representation of Volusia County" (2024). *Doctoral Dissertations and Master's Theses*. 844.
<https://commons.erau.edu/edt/844>

This Thesis - Open Access is brought to you for free and open access by Scholarly Commons. It has been accepted for inclusion in Doctoral Dissertations and Master's Theses by an authorized administrator of Scholarly Commons. For more information, please contact commons@erau.edu.

**Refinement of a Regional Storm Surge Mesh for High-Resolution Topographic
Representation of Volusia County**

By
Morgan Tanner Harbin

A Thesis Submitted to the College of Engineering Department of Civil
Engineering in Partial Fulfillment of the Requirements for the Degree of
Master of Science in Civil Engineering, Environmental Sustainability and Resilience

Embry-Riddle Aeronautical University
Daytona Beach, Florida
August 2024

I. ACKNOWLEDGEMENTS

This thesis was made possible by the generous support of Embry-Riddle Aeronautical University through the FIRST Grant for graduate research as well as by the NASA MUREP DEAP project funded by the National Aeronautics and Space Administration (80NSSC23M0053). Its contents are solely the responsibility of the award recipient and do not necessarily represent the official views of the funding agencies. Many thanks go to the Civil Engineering department at Embry-Riddle Aeronautical University here in Daytona Beach as well as to the university at large; both parties have ensured my financial ability to graduate with this Masters of Civil Engineering.

The research presented herein and the professional development of myself, the author, are the fruits of not only 2 years of my own concerted effort but also the decades of focused curiosity Dr. Medeiros has committed himself to for the advancement of research in coastal hydraulics and stormwater management. His professional strengths straddle the intersections of applied engineering practice, theoretical understanding, and advanced technology application, and his research approach is one of great integrity and sincerity, thereby earning his reputation as an effective favorite here at Embry-Riddle. The Civil Engineering department would certainly not be the same without him, and the same speculation can be made of my professional life: my organizational approach, fieldwork capabilities, critical thinking skills, technological understanding, and of course, my thesis, would never have developed without his patient teaching.

For all his investment in me, Dr. Medeiros didn't have to bear the burden of this stressed student at home; instead, I have my wife, Alyssa Harbin, to thank for that. She sacrificed the stabilities of a focused and calm household in turn for the crazed lifestyle of me whizzing in and out between school and work, all while pursuing her own master's degree as a full-time teacher. I thank her for this as well as for the jovial adventures she has joined me on these past 5 years

together, many of which she ventured on selflessly. She would agree that I also owe a great debt to the investments of my father, mother, sister, and extended family for their prior decades of investment in my varied interests. I thank my father that he attuned me towards details, minor and major, in my work and thereby exhorted me to be a reliable and competent man, both professionally and personally; I thank my mother for raising me on her sweet enthusiasm and undeniable care, which has certainly kept my sane throughout my education and my life; and I thank my sister for always reminding me to laugh and to keep life in perspective, and when I forget to laugh, she just makes me!

Read on, and see the fruits of their investment.

II. ABSTRACT

In 2022, Volusia and Flagler Counties of northeast central Florida were impacted indirectly by consecutive Hurricanes Ian and Nicole; the destabilization of dunes and armoring infrastructure caused by Ian left the region susceptible to Hurricane Nicole, which caused unprecedented coastal damage to dunes and seawalls. The extent of damage that occurred within Volusia and Flagler Counties during the 2022 hurricane season, the underrepresentation of this region within sustainability and resilience research, and the ecological, social, and economic value of the geography provide just cause for scientific inquiry of the area's coastal dynamics. This thesis specifically describes an investigation of Hurricane Ian's impact on Volusia County by means of numerical modeling. The heavily validated ADvanced CIRCulation (ADCIRC) numerical model, which synthesizes vertically-integrated equations of mass and momentum into a generalized wave-continuity equation (GWCE), thereby producing solutions to shallow water equations, was used to simulate Hurricane Ian's tidal and meteorological patterns over the domain of a refined mesh. The FLAgler VOLusia highResolution (FLAVOR) mesh was developed by paving a sub-mesh to a resolution of 50 m along the path of Volusia County's seawalls and merging this with the validated HSOFS mesh. FLAVOR model performance across both tidal and meteorological simulations of Hurricane Ian was close to that of HSOFS and produced a satisfactorily greater inundation extent than that modeled by HSOFS along Volusia County's coast, providing more precise metrics regarding the surface water elevation and surge velocity close to Volusia County's seawalls. This model output, as well as output produced by successive refinements of the FLAVOR mesh, may be used to hindcast a variety of tropical cyclones and to forecast future coastal events for Volusia and Flagler Counties' informed decision making in the realms of policy creation, evacuation coordination, stormwater management, and resilient design.

III. TABLE OF CONTENTS

I.	Acknowledgements	2
II.	Abstract.....	4
III.	Table of Contents.....	5
IV.	List of Figures.....	6
V.	List of Tables	8
VI.	Nomenclature.....	9
VII.	Introduction	11
VIII.	Hurricanes Ian and Nicole	15
IX.	Storm Surge Modeling.....	21
X.	Mesh Development.....	28
XI.	Model Development	32
XII.	Mesh & Model Validation.....	37
XIII.	Results	40
	Elevation	40
	<i>NOAA Tidal Station Time Series Analysis</i>	40
	<i>Peak Value Analysis</i>	44
	Velocity	46
	<i>Bootstrapping</i>	46
	<i>Visual Analysis</i>	48
XIV.	Conclusions and Recommendations	56
XV.	References	58
XVI.	Publications	64

IV. LIST OF FIGURES

Figure 1 delineates the paths of Hurricanes Ian and Nicole, the cones of which passed through Volusia County on September 28th, 2022, respectively. Damage resulting from the combined effect of both storms was on the order of \$500 million despite both impacting.....14

Figure 2 contextualizes erosion throughout Florida resulting from the combined effect of Ian and Nicole; erosion conditions range from 0 (no impact) to IV (severe). Much of Volusia County’s coast experienced erosive condition IV, particularly along the populous.....19

Figure 3 illustrates the relationship between mesh resolution and wetting/drying algorithm. It can be observed that a fine resolution mesh would result in more accurate “wetted” cells and would decrease the occurrence of artificially dry areas. The improvement of.....25

Figure 4 demonstrates the benefit of increased mesh resolution as a beach profile. From the ocean (right) to the land (left), it can be observed that an increased resolution, similar to that implemented in FLAVOR, can provide up to 10 times more elevation points for.....28

Figure 5 displays the HSOFS mesh in its full domain, stretching from the 65-degree W meridian (right) to the east coast of North and South Americas. Puerto Rico is enlarged (left) for detail; note the triangular mesh elements that vary in proportion and size.....30

Figure 6 displays the HSOFS mesh (left) and the FLAVOR mesh (right) overlaid atop an aerial of Daytona Beach. The HSOFS resolution is 300 to 400 m in this area, while FLAVOR provides a resolution of approximately 50 m along the seawall.....30

Figure 7 demonstrates the oscillatory pattern of water surface elevation across a FLAVOR model run with only tidal forcings. These oscillations are shown atop observations provided by NOAA from the tidal station located in Mayport, FL. Note the spring tide, in.....31

Figure 8 contextualizes the 5 NOAA stations used for model validation in relation to the Volusia County coastline of interest (yellow polygon).....37

Figure 9 demonstrates FLAVOR agreement with observed data recorded at 5 NOAA Tides and Currents stations for a meteorological simulation of Hurricane Ian. The first 4 of these are located coastally, while the I-295 Buckman Bridge station is located on.....41

Figure 10 demonstrates HSOFS agreement with observed data recorded at 5 NOAA Tides and Currents stations for a meteorological simulation of Hurricane Ian. The first 4 of these are located coastally, while the I-295 Buckman Bridge station is located on.....42

Figure 11 shows a Florida Department of Environmental Protection (2022) employee indicating the approximate height of a stain line left by Hurricane Ian in Naples, FL. Note the roughly ½ foot width of the stain line; this broadness results in ambiguity of measurement.....44

Figure 12 compares HSOFS and FLAVOR velocity results following the bootstrap operation performed on the non-Gaussian datasets. The operation confirms that FLAVOR mean coastal velocities lie outside 2 standard deviations of the HSOFS mean.....46

Figure 13 rasterizes velocity differences between HSOFS and FLAVOR output in the domain of refinement of FLAVOR. Significant differences occur in estuarine and tidal flat regions.....47

Figure 14 represents the 10 locations at which citizen photographs were taken and submitted anonymously to ERAU. Locations represent a range of infrastructural purposes, such as high-density residential (i.e., condominiums) to public spaces.....49

Figure 15 illustrates surge extent, elevation, and velocity upon approach towards the seawall at Frank Rendon Park, a public facility with parking and playground amenities. Note the finer resolution of FLAVOR output and input as well as the greater surge extent.....51

Figure 16 illustrates surge extent, elevation, and velocity upon approach towards a home in Wilbur-By-The-Sea, a residential area made famous for the homes that collapsed into the Atlantic following hurricane Nicole. Note the finer resolution of FLAVOR output.....52

Figure 17 illustrates surge extent, elevation, and velocity upon approach towards the seawall at 10 locations throughout Daytona Beach Shores. The distance between modeled surge extent, maximum surface water elevation along profile line, and maximum.....54

V. LIST OF TABLES

Table 1 tabulates statewide damage resulting from hurricanes Ian and Nicole in the 2022 Floridian hurricane season. Aside from Lee County, which experienced the direct impact of Hurricane Ian as a Category 4 hurricane, Volusia County experienced..... 15

Table 2 compares armoring (seawall and other surge-dissipating infrastructure) damage across Florida. Volusia County ultimately experienced 4.98 miles of armoring loss (including both minor and major), the greatest stretch of any Floridian county during the 2022 hurricane season..... 17

Table 3 quantifies erosion throughout Florida resulting from the combined effect of Ian and Nicole; erosion conditions range from 0 (no impact) to IV (severe). Volusia County experienced a total of 38 eroded miles of coast (74% of which constituted..... 18

Table 4 describes the input files required to run an ADCIRC model. The fort.14 and fort.15 files are required under all circumstances, and the fort.13 and fort.22 files are conditionally required; their inclusion is dependent upon the parameters defined in the fort.15 file..... 21

Table 5 summarizes the 8 primary tidal constituents used to force the FLAVOR model in both the tides-only incremental validation as well as the meteorologically-forced final variation..... 33

Table 6 compares HSOFS and FLAVOR elevation results to true elevation. Elevation data within the FLAVOR domain was difficult to obtain and predominantly unconsidered in this chart. Stations colored red in the “Vicinity” column are outside the boundaries of Volusia County..... 43

VI. NOMENCLATURE

ADCIRC	ADvanced CIRCulation coastal surge model
AGL	Above Ground Level
ArcMap	GIS computer program produced by ESRI
ESTOFS	Extratropical Surge and Tide Operational Forecast System
FDEP	Florida Department of Environmental Protection
FEMA	Federal Emergency Management Agency
FLAVOR	FLAgler VOlusia highResolution mesh
GWCE	Generalized Wave Continuity Equation
HSOFS	Hurricane On-Demand Forecast System
HWM	High-Water Mark
MAE	Mean Absolute Error
MAPE	Mean Absolute Percentage Error
NMB	Normalized Mean Bias
NOAA	National Oceanic and Atmospheric Administration
NOS	National Ocean Service, a division of NOAA
Raster	Computer image for which pixels represent values

R ²	Regression coefficient
RMSE	Root Mean Square Error
RTK-GNSS	Real Time Kinematic Global Navigation Satellite System survey method
SAB	South Atlantic Bight mesh
SLAMM	Sea Level Affecting Salt Marshes Model
SLOSH	Sea Lakes and Overland Surges from Hurricanes model
SMS	Surface-water Modeling System
USGS	United States Geological Survey
WD	Wetting/Drying algorithm

VII. INTRODUCTION

Following substantial destruction in Fort Myers beach resulting from Hurricane Ian's 2022 landfall, Ian's path passed the Floridian peninsula to the northeast and impacted central Florida's coast as it crossed into the Atlantic 100 km south of Volusia County and dissipated upon landfall in South Carolina. Within the following month, central Florida's coast was impacted from the east by Hurricane Nicole, which wrought disproportionately severe damage in Volusia County for a category 1 landfall (Abbott, 2023) roughly 180 kilometers south (NOAA Nicole Summary). Dunes eroded, seawalls failed, and pool decks collapsed due to the hurricane's impact on a coast already compromised by Ian.

According to scientific literature, these impacts are predominantly attributed to storm surge, which constitutes the vertical rise and horizontal travel of tidal waters over the course of a tropical cyclone; it is distinguished from other elements of hurricane impact including but not limited to meteorology (i.e., wind, pressure, and rainfall) and wave action (i.e., short-period vertical and horizontal undulation of water resulting from wind). Topobathymetry, the elevation characterization of a domain encompassing both inland (topographic) and underwater (bathymetric) surfaces, is the primary influence of surge extent and can be understood in terms of surge interaction with surface geometry as dictated by gravity. Vertical features, including coastal roadways, buildings, and seawalls, direct or dampen surge and create turbulence; the more slender of these features (i.e., seawalls or coastal roads) are often unrepresented in computational surge models due to their sub-resolution width (Coggin, 2008). Inland watercourses, including ditches, canals, rivers, or intracoastal waterways, provide channels through which surge can flow; these influence the spread of surge by distributing it throughout a domain. These features are all

interrelated within a given domain and as a network influence the routing, elevation, and velocity of surge.

The human response to storm surge has implications for both ecological preservation and anthropogenic development. Several unique ecosystems span the coastal region of east central Florida and are influenced in their development by storm surge dynamics. A study of ecosystem services indicated estuaries and seagrass to be the most effective cyclers of nutrients, tidal marshes and mangroves to be the most substantial natural treater of waste and xenic nutrients, and estuaries to be a substantial contributor to wildlife refuge and recreational value (Costanza *et al.*, 1998). Each of these environments exists along Volusia County's coast. The saltmarsh in particular is a crucial dissipator of storm surge (Medeiros, Bobinsky, and Abdelwahab, 2022) and tidal flow (Alizad *et al.*, 2015) in Florida and flourishes in large swaths due to the micro to mesotidal patterns along Florida's coast. Its dynamics, from sedimentation and growth to migration and surge dissipation, are of interest to local resilience efforts, particularly as the migration of salt marshes is restricted by coastal development (Enwright, Griffith, and Osland, 2016). A study in the Virginia Coast Reserve reported that the narrow elevation band that allows for regular inundation without saltmarsh drowning is conducive to dissipation of tide and wave energy. The east central Florida coast lies within a transitional region between micro and mesotidal patterns, and saltmarsh dissipation of tide and wave action is therefore maximized here (Short, 1991; de Groot, Veeneklaas, and Bakker, 2011). In the event of strong surge, saltmarshes are exposed to increased lateral stresses as well as allochthonous coarse-grain sand deposition. Due to the typical fine-grained sediments in the saltmarsh rhizome complex, coarse grain depositions are generally not conducive to saltmarsh growth in excess but can provide additional foundation in moderation. The prevalence of dunes and tidal flats in Volusia County (particularly in the Halifax Urban Watershed)

makes the region prone to over wash, and the local saltmarsh environment receives this sediment during surge events. Hurricanes Ian and Nicole likely carried this sediment to the surrounding saltmarshes in addition to the sediment conveyed as a result of seawall destruction and subsequent washout of the sandy foundations. Man-made structures, channel connectivity, and topography all impact the dynamics of sediment transport during storm surge inundation; moreover, the dynamic evolution of surge resulting from sea-level rise and salt marsh migration, the latter of which dictates bottom friction and therefore the extent and energy of storm surge (Bilskie *et al.*, 2016), requires high-resolution surge elevation and velocity data. It is therefore critical to consider these elements throughout the development of a computational surge model.

Man-made structures exert varying influence upon surge-induced inundation depending on their state of operation. Seawalls, for example, work effectively to dampen surge velocity and deflect wave energy in their designed state, but compromised seawalls leave coastal foundations vulnerable to washout and collapse. Seawalls fail due to a combination of pressures from inside the seawall mainly due to increased soil saturation and density as well as decreased shear stresses during surge backwash (Takahashi *et al.*, 2022).

Flood studies indicate high risks for structures directly on the coast, with most damage occurring on the coastal side and on the first floor of the structure due to the high landward winds and ground-level surge produced during tropical cyclones. Damage costs generally display an inversely-proportionate relationship to distance from shore (Xian, Lin, and Hatzikyriakou, 2015). As the 3rd most-populous state in the United States of America and a notable host of coast-bound tourists, Florida has developed into a profitable hub for commerce and a rewarding home for Americans seeking a range of lifestyles. Approximately 76.5% of its residents live within coastal zones prone to impact by tropical cyclones (National Oceanic and Atmospheric Administration).

In Volusia County, roughly 55 km of its 80 km coastline, as measured in ArcMap for this research, are developed directly on or across the street from the shoreline with condominiums, businesses, and residences. Once destroyed, these coastal structures may leave landward located structures exposed to the full power of wind gusts and surge. Moreover, the force of surge is compounded by the presence of structural debris, and all structures downstream of the surge are susceptible to enhanced damage in this scenario.

Global discussion of climate change, a phenomenon predicted and observed to have increased the intensity of meteorological events (Bender *et al.*, 2010) as well as the average temperature of the atmosphere and hydrosphere (Catto, Shaffrey, and Hodges, 2001), underscores the necessity of bolstered infrastructure against natural disaster and has prompted Florida, the site of atmospheric and hydrological phenomena ranging from the daily storms of the summer months to the intense wave action of the winter months, to incorporate the concept of resiliency into its policies and designs. Resiliency, defined as the ability to anticipatorily prepare for and reactionarily recover from disaster in such a way that a system may return to its previous functionality (Zaccarelli, Petrosillo, and Zurlini, 2008), is addressed bilaterally: immediate prosperity of human life is protected by monitoring and preparing for disaster, while perpetual prosperity is made resilient and sustainable by developing infrastructure from designs informed by validated scientific observation and modeling.

VIII. HURRICANES IAN AND NICOLE

The hurricane season of 2022 exposed shortcomings in the resilient infrastructure of Volusia County. Subsequent hurricanes Ian and Nicole made landfall within 6 weeks of each other, resulting in substantial loss of property and approximately \$500 million in damage within Volusia County. Ian is most known for its impact on southwest Florida, which experienced the leveling of Ft. Myers beach, washout of causeways, wide swaths of flooding, and severe erosion of Sanibel and Pine Islands. Of the Floridian counties outside Lee County, Volusia County suffered most loss during the 2022 hurricane season (Florida Department of Environmental Protection, 2022); a tabulation of infrastructure damage is available in Table 1. The paths of both hurricanes, neither of which cross within 50 km of Volusia County, can be seen in Figure 1 alongside damage photographs from Volusia County.

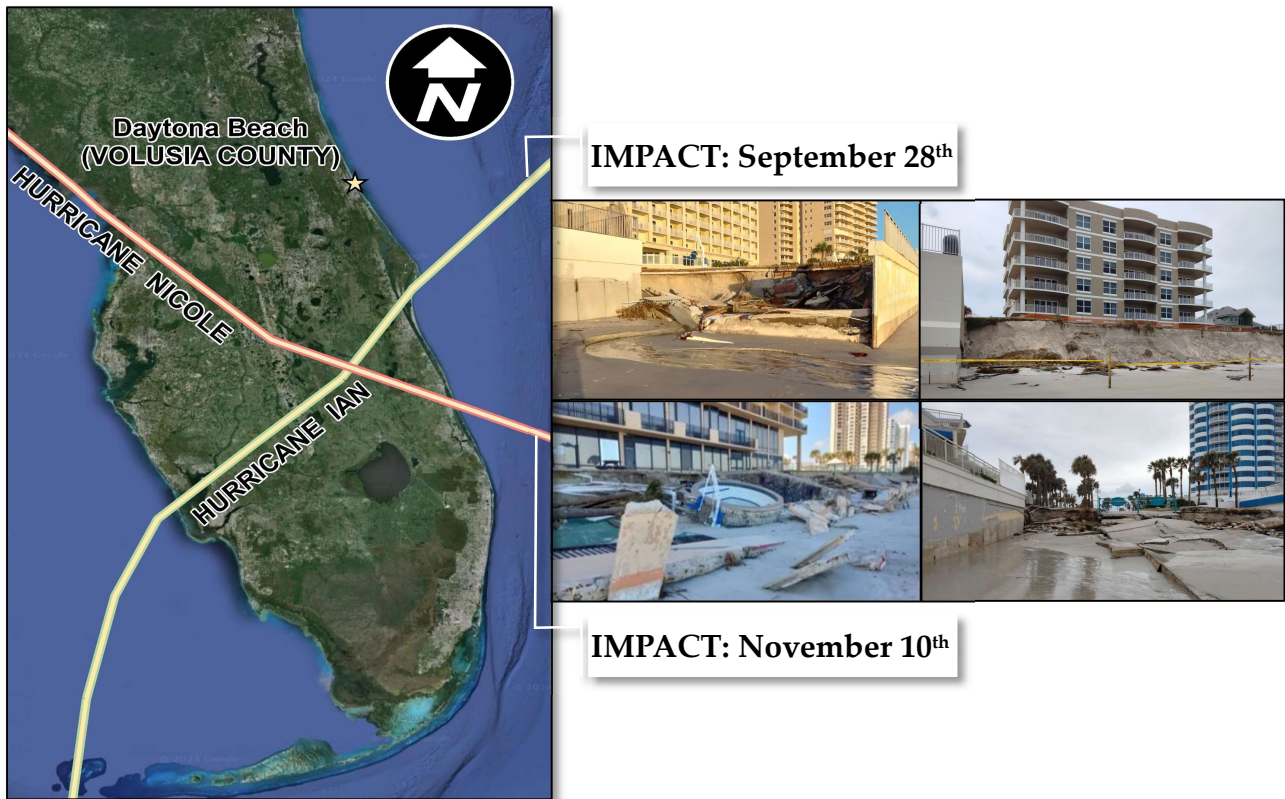


Figure 1 delineates the paths of Hurricanes Ian and Nicole, the cones of which passed through Volusia County on September 28th, 2022, respectively. Damage resulting from the combined effect of both storms was on the order of \$500 million despite both impacting Volusia County non-directly and as a Category 1 hurricane and tropical storm, respectively. Right: citizen photos, anonymous by request.

Table 1 tabulates statewide damage resulting from hurricanes Ian and Nicole in the 2022 Floridian hurricane season. Aside from Lee County, which experienced the direct impact of Hurricane Ian as a Category 4 hurricane, Volusia County experienced the greatest loss of infrastructure despite the indirect hit of both hurricanes. Brevard, Indian River, and Broward counties all are located closer to the paths of both storms (Florida Department of Environmental Protection, 2022).

STRUCTURAL DAMAGE INCURRED BY HURRICANES IAN AND NICOLE BY COUNTY

HURRICANE IAN MAJOR STRUCTURAL DAMAGE				
County	Number of Single-Family Dwellings Damaged	Number of Multi-Family Dwellings Damaged	Number of Other Major Structures Damaged	Total Number Damaged
Volusia	272	68	24	364
Sarasota	32	12	1	45
Charlotte	156	62	5	223
Lee	2,791	502	220	3,513
Collier	173	69	20	262
St. Johns	16	3	0	19
Flagler	61	5	10	76
TOTAL	3,501	721	280	4,502

HURRICANE NICOLE MAJOR STRUCTURAL DAMAGE				
County	Number of Single-Family Dwellings Damaged	Number of Multi-Family Dwellings Damaged	Number of Other Major Structures Damaged	Total Number Damaged
Volusia	35	12	62	109
St. Johns	10	2	1	13
Flagler	7	1	1	9
Brevard	14	3	2	19
Indian River	2	3	2	7
Broward	0	0	1	1
TOTAL	68	21	69	158

Both Hurricanes Ian and Nicole followed a path through Florida’s east coast south of Volusia County; Ian developed throughout the Caribbean and crossed from Lee County to Cape Canaveral, impacting Volusia County on the night of September 28th, 2022, and Nicole developed in the Atlantic and made landfall in Vero Beach on November 10th of the same year. During Ian, storm surge on the southwest coast reached 10 to 15 ft above ground level (AGL) and in Volusia County reached 3 to 5 ft AGL. Despite its indirect hit, Ian’s impact resulted in greater damage to

buildings than at any other point in the past half century of Volusia County's history (Florida Department of Environmental Protection, 2022); in total, Volusia County sustained 364 major structural damages.

Several factors, including strength of reinforcing steel, wall thickness, age, and increased soil pressure on seawalls resulting from the erosion of beach sand contributed to 1.85 miles of major and minor destruction of Volusia County armoring infrastructure (revetments, seawalls, etc.) following Ian and left several seawalls in such condition that substantial rainfall would likely cause failure. Total armoring loss in Volusia County was greater than that of Lee County. Approximately 1 ½ months later, Hurricane Nicole indirectly impacted Volusia County. Weakened seawalls, strained stormwater systems, and the slowly-receding St. John's River watershed flooding, impacts wrought by Hurricane Ian, compounded the damage Nicole would have done in isolation. This second storm destroyed 3.13 miles of seawall in Volusia County, and the total loss of 4.98 miles of armoring represented the most substantial economic impact to Volusia County between both hurricanes. Total armoring damages for both hurricanes are shown in Table 2. It should be noted that less of this destruction occurred in the southern part of Volusia County; this is likely due to the fact that the City of New Smyrna Beach had updated its armoring following Hurricane Jeanne in 2004, whereas the City of Daytona Beach and surrounding municipalities did not do the same. Structural damages in Volusia County far exceeded those of other counties following Nicole; Volusia experienced 109 major damages, while the county of 2nd greatest destruction, Brevard, experienced 19 major structural damages. Substantial erosion from both storms lowered the beach profile by 2-5 feet countywide, resulting in enhanced soil pressures exerted on seawalls.

Table 2 compares armoring (seawall and other surge-dissipating infrastructure) damage across Florida. Volusia County ultimately experienced 4.98 miles of armoring loss (including both minor and major), the greatest stretch of any Floridian county during the 2022 hurricane season.

ARMORING DAMAGE INCURRED BY HURRICANES IAN AND NICOLE BY COUNTY

HURRICANE IAN ARMORING DAMAGE		
County	Major Damage (Feet)	Minor Damage (Feet)
Lee	4,756	1,525
Collier	3,036	0
St. John's	0	845
Flagler	1,200	9,350
Volusia	6,330	3,435
TOTAL (Feet)	15,322	15,155
TOTAL (Miles)	2.90	2.87

HURRICANE NICOLE ARMORING DAMAGE		
County	Major Damage (Feet)	Minor Damage (Feet)
St. John's	2,008	1,243
Flagler	7,790	2,036
Volusia	13,262	3,265
TOTAL (Feet)	23,060	6,544
TOTAL (Miles)	4.37	1.24

The combined effect of both hurricanes eroded between 10 to 18 cubic yards for each foot of coastline between New Smyrna Beach (south) and Ormond Beach (north). The Florida Department of Environmental Protection ranks erosive conditions on a scale of I through IV, with IV representing severe erosion on the scale of dune washout and seawall destruction; Figure 2 maps these conditions along Volusia County’s coast, of which the majority was deemed erosive condition IV (2022). The extreme scale of erosion is attributed to the destabilization of the

coastline from Ian’s impact and the wide wind field, 40 miles in radius, of Hurricane Nicole. Though only rated a Category 1 storm upon impact, Nicole was reported to have generated Category 4/5 wave heights of around 32 ft between 20 and 120 nautical miles off Cape Canaveral’s coast (Florida Department of Environmental Protection, 2022). The damage incurred by these storms, seemingly disproportionate to the intensity and proximity of their impacts to Volusia County, is cause for investigation into the behavior of storm surge related to these events. In this research, such an investigation is undertaken by developing a surge model and hindcasting Hurricane Ian.

Table 3 quantifies erosion throughout Florida resulting from the combined effect of Ian and Nicole; erosion conditions range from 0 (no impact) to IV (severe). Volusia County experienced a total of 38 eroded miles of coast (74% of which constituted severe, type IV erosion) (Florida Department of Environmental Protection, 2022).

COUNTY	EROSION CONDITIONS (miles)					
	0	I	II	III	IV	Total
COLLIER		7			58	65
LEE		0	10	1	32	43
BREVARD		5	14	10	10	39
ST. JOHNS		2	10	6	21	39
VOLUSIA		2	3	5	28	38
SARASOTA	5	19				25
MARTIN	2	2	17	2		23
INDIAN RIVER		4	5	5	8	22
ST. LUCIE	5	11	4	2		22
FLAGLER		1	5	3	9	19
CHARLOTTE		4	2			6
TOTAL	12	59	70	34	167	341

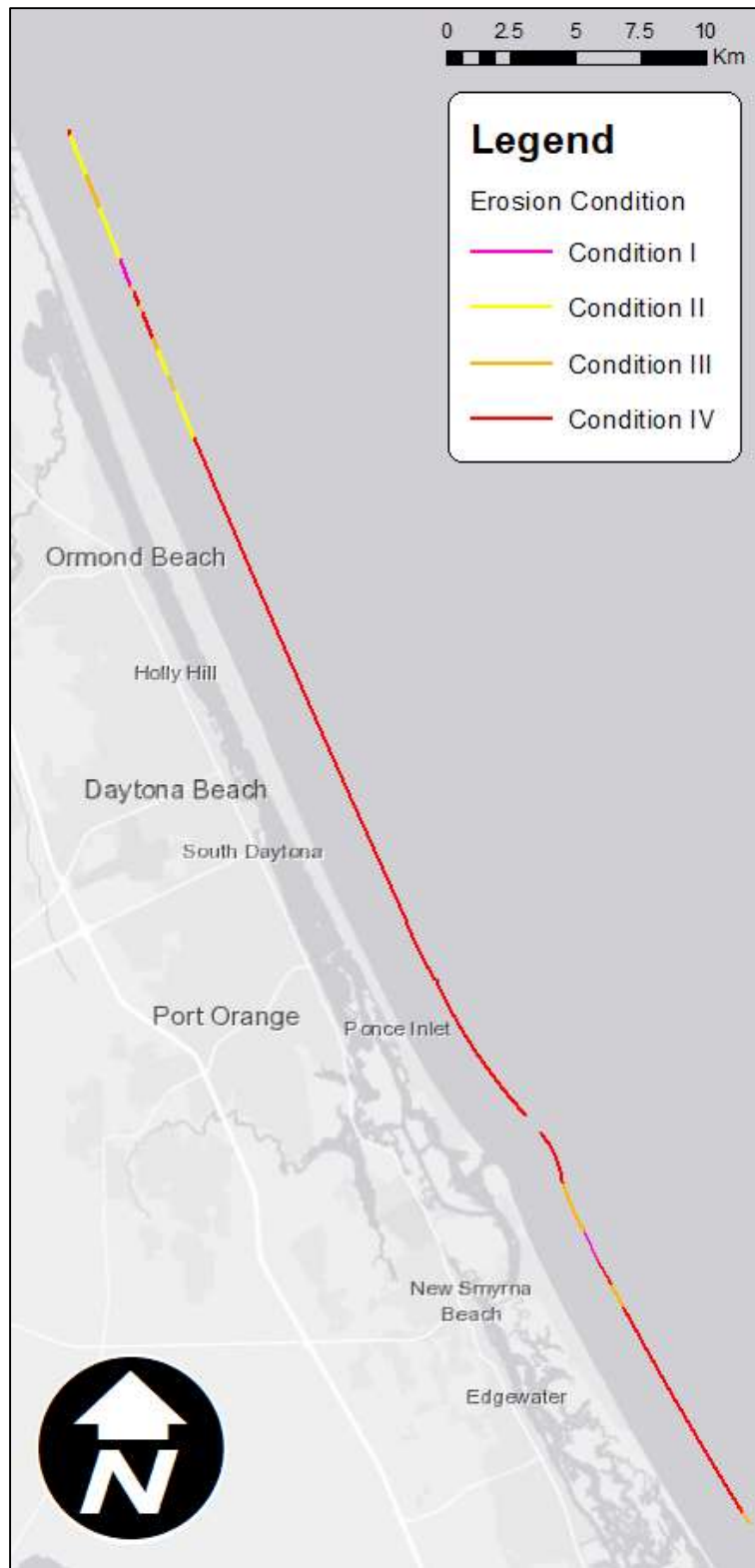


Figure 2 contextualizes erosion throughout Florida resulting from the combined effect of Ian and Nicole; erosion conditions range from 0 (no impact) to IV (severe). Much of Volusia County's coast experienced erosive condition IV, particularly along the populous central strand running south from Ponce Inlet to Ormond Beach in the North (Florida Department of Environmental Protection, 2022).

IX. STORM SURGE MODELING

The ADCIRC-2DDI (ADvanced CIRCulation) numerical modeling code uses a two-dimensional, depth integrated approach to ocean circulation modeling; inputs to the model are tabulated in Table 4 (Luettich, Westerink, and Scheffner, 1992). ADCIRC synthesizes vertically-integrated equations of mass and momentum into a generalized wave-continuity equation (GWCE), which produce solutions to shallow water equations. Along with the GWCE, non-conservative momentum equations are carried out over an unstructured, triangular, finite element mesh used to discretize the domain and are solved using a standard Galerkin method (Funakoshi, Hagen, and Bacopoulos, 2008). The mesh is used to define the spatial resolution of the ADCIRC model and therefore impacts the level of detail and accuracy of ADCIRC output. Mesh development approaches generally try to minimize computational cost by increasing resolution in areas of interest and relaxing it in areas where solution gradients are relatively consistent (Thomas, Dietrich, Dawson, and Luettich, 2022). ADCIRC has been historically used for research into the impacts of tidal phase on surge and wave action (Marsooli and Lin, 2018), significance of representing vertical features in surge models (Bilskie *et al.*, 2015), and interaction between wind-induced waves and storm surge (Dietrich *et al.*, 2010). The work outlined in this thesis utilizes the ADCIRC model in order to test and validate a refined mesh for the coast of Volusia County in NE Central Florida.

Table 4 describes the input files required to run an ADCIRC model. The fort.14 and fort.15 files are required under all circumstances, and the fort.13 and fort.22 files are conditionally required; their inclusion is dependent upon the parameters defined in the fort.15 file. Files are loaded into a single directory and executed from the command-line interface (CLI) of a high-performance computer (HPC).

FILE	ADCIRC MODEL INPUTS		
	FILE TYPE	FILE CONTENTS	REQUIREMENT
fort.13	Nodal Attributes File	Numeric descriptions of node attributes that only vary in space.	CONDITIONAL
fort.14	Grid and Boundary Information File	Coordinates and elevation values for nodes of a given mesh.	REQUIRED
fort.15	Model Parameter and Periodic Boundary Condition File	Parameterized model attributes including bottom friction, tidal input, ocean circulation, etc.	REQUIRED
fort.22	Meteorological Forcing Data File	Time and space defined file that incorporates elements such as wind speed and storm trajectory depending on which of 20 NWS variants are selected.	CONDITIONAL

Existing studies in this vicinity address SLR-induced saltmarsh migration using the Sea Level Affecting Marshes Model (SLAMM) (Linhoss, Kiker, Shirley, and Frank, 2015) or social response, including resident perception and evacuation routes, to Volusia County flooding events using the Sea Lakes and Overland Surges from Hurricanes (SLOSH) model (Helderop and Grubestic, 2018). The latter of these more closely resembles the study proposed in this thesis, but even so, Helderop and Grubestic’s research assumes the accuracy of existing flood modeling in Volusia County. On the contrary, this thesis acknowledges existing deficiencies as a result of insufficient local parametrization of the ADCIRC model (Dietrich *et al.*, 2012) or of surge underestimation in the case of the SLOSH model and seeks to mitigate ADCIRC modeling errors with increased mesh resolution.

Specifically, this thesis proposes the long-term development and refinement of a coastal flood model suitable for Volusia County. The initial research for this long-term project requires localized refinement of the Hurricane Surge On-demand Forecast System (HSOFS) mesh. HSOFS

was developed to be a rapidly-deployable (i.e., computationally-efficient) hydrodynamic model; the HSOFS mesh utilizes a coarse-resolution nodal arrangement and produces results with an average RMSE of 0.26 meters across a series of 10 hindcasted hurricanes used for model validation (Riverside Technology Inc. & AECOM, 2015).

The long-term objective for this thesis is to establish a modified variant of HSOFS that refines mesh resolution for the Volusia County area and incorporates current topobathymetry using elevation data from NOAA's Digital Coast and from Real-Time Kinematic Global Navigation Satellite System (RTK-GNSS) ground-truth measurements in areas of critical topography. ADCIRC simulations using this refined mesh, referred to as the FLAgler VOLusia highResolution (FLAVOR) mesh, were executed for Hurricane Ian, the results of which were compared to true inundation measurements. In doing so, this research will answer the call for further research by providing Volusia County with a research grade mesh which will produce more localized results, enabling more informed decisions regarding infrastructural development. FLAVOR refinement focuses on Volusia County at present but will be expanded to represent Flagler County in the future.

Generalized coastal meshes, especially those developed for near-real time forecasting, do not normally reach below 100 m resolution; previous discussions of the balance between mesh resolution and computational efficiency often echo those of Lin *et al.* (2012), who found a 100 m mesh resolution to produce sufficiently accurate results as compared to a ~10 m mesh used by Colle *et al.* (2008) and therefore sacrificed 2.5% accuracy for more efficient computing. Arguments like those of Colle are contextually correct, as models of large domain such as those observed in Colle's paper are not developed for hyper-local surge predictions. However, considering the localized objectives of this thesis, it is asserted here that these considerations and novelties justify the effort of producing a research-grade mesh for Volusia County, Florida.

This ability of a flood model to represent the nuances of local geography and topography through the refinement of its base mesh is fundamental to the pursuit of accuracy. A variety of meshes exist at present to represent the Eastern US, each developed with a specialized goal. The Hurricane Surge On-demand Forecast System (HSOFS), for example, was developed as a rapidly deployable (i.e., computationally efficient) mesh to be used to forecast storm surge in emergency scenarios as storms propagate (Riverside Technology Inc. & AECOM, 2015). Its large domain allows for application from the 65° W meridian to all coastal swaths across the Eastern Seaboard as well as the Gulf Coast of Mexico, and its resolution, reaching 150 m in its finest areas, allows for acceptable accuracy for the determination of evacuation procedures.

Most discussion of mesh resolution reflects that asserted by Hu *et al.* (2018) that detailed resolution (and therefore topographic representation) is to be used sparingly, only where and when needed to represent hydraulically significant features, in the interest of computational efficiency, which is one of the main advantages of the unstructured triangular mesh approach used by ADCIRC. Thomas *et al.* (2022) directly explored the quantifiable impact of mesh resolution, thereby electing to incorporate enhanced resolution and topography not sparingly but instead thoroughly, by comparing 2 meshes: the aforementioned HSOFS mesh and the South Atlantic Bight mesh, the latter of which is a high-resolution (“production-grade”) mosaic of FEMA regional meshes. Thomas *et al.* produced a statistical analysis of both meshes’ performance in simulating Hurricanes Matthew and Florence as compared to ground observation inundation measurements derived from NOAA tidal stations and USGS high-water marks. These hurricanes were strategically selected for their unique shore-parallel and shore-normal impacts, which are proven to produce different patterns of inundation. The study’s results demonstrated more accurate inundation measurements (depth and velocity) by the finer SAB mesh in computations of best-fit

slope, regression coefficient (R^2), root mean square error (RMSE), and normalized mean bias (NMB) relative to *in-situ* data provided by NOAA and USGS; furthermore, the SAB mesh demonstrated a significantly greater flood extent than that of HSOFS as a result of its representation of hydraulic features. Therefore, the output of a fine mesh such as the SAB mesh has greater potential to be integrated into inland models of flood-conveyance than the coarse HSOFS and provides hyper-localized results that allow for analysis of specific hydraulic systems.

The importance of mesh resolution is underscored when considering the wetting and drying algorithm, a fundamental component of flood models; this dictates the computational domain for a given time step by categorizing mesh elements as wet or dry (or partially-wet, depending on the algorithm) using a variety of criteria. A thorough review of WD algorithms was presented by Medeiros and Hagen (2013). ADCIRC uses a “depth threshold” method that categorizes a mesh element “wet” if inundation exceeds a preset depth specified in the model control file (fort.15). Figure 3 illustrates the relationship between WD algorithm and mesh resolution as depicted by Medeiros and Hagen (2012); one can observe that a cell may be categorized “wet” as a result of a wetting threshold being surpassed in the element area; in the case of a coarse resolution mesh, an element representing a large area may be categorized as dry, whereas the same area comprised of fine resolution elements would be more precisely distinguish each element as “wet” or “dry,” providing finer spatial output for surge velocity and elevation and therefore finer detail for purposes of urban management, hydraulic construction, ecological management, and evacuation

planning. As this thesis is intent on providing a scalable mesh for the area of interest, it is prudent to develop a topographically informed mesh that produces strong statistical correlation with *in-situ* inundation measurements and one that is developed such that is capable of near-seamless integration with complementary models of inland hydraulics.

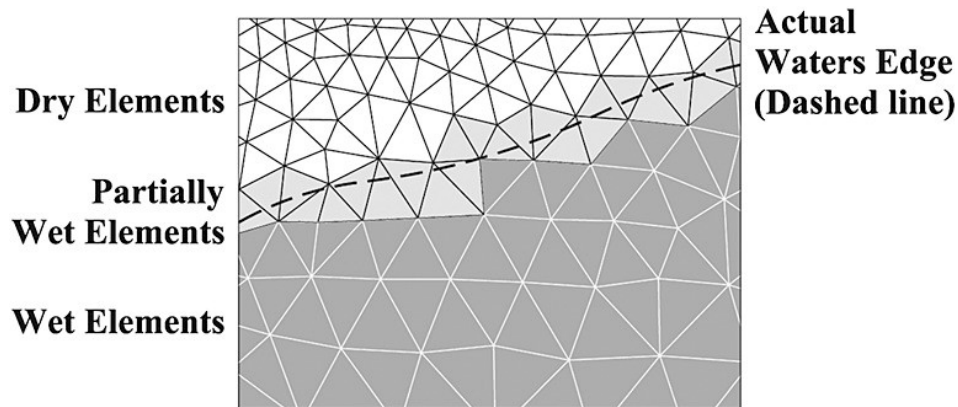


Figure 3 illustrates the relationship between mesh resolution and wetting/drying algorithm. It can be observed that a fine resolution mesh would result in more accurate “wetted” cells and would decrease the occurrence of artificially dry areas. The improvement of finer resolution would give emergency managers, engineers, and scientists more accurate information for the design of evacuation routes, infrastructure, and conservation tactics. (Medeiros and Hagen, 2012)

The novelty of this research lies in the topographically informed mesh refinement representing the northern Floridian urban watershed enveloped by Volusia County, one that has not yet been investigated using the extensively validated ADCIRC model. Given its spatial variability of elevation, bottom friction, and other pertinent modeling attributes, the variety of ecosystems present in and around the Halifax Urban watershed, the substantial destruction Volusia County has incurred in recent years, and the anticipated changes in climate that will certainly affect the low-lying natural coast of Volusia County as well as its abundance of coastal infrastructure, the refined ADCIRC model proposed here will provide the first purposeful investigation into the elevation and velocity of storm surge produced in this region. Resiliency and sustainability are core motivations for this thesis: the exhaustive rebuilding efforts that residents of Volusia County have undertaken not only following Hurricanes Ian and Nicole of 2022 but also following the likes of Hurricanes Irma (2017) and Matthew (2016) have represented substantial economic loss and

material waste, and the time spent making reparations represents a loss of profitable time for the community. Storefront building supplies, seawall pilings and cement caps, residential commodities, and commercial time may be saved in the future if the research described herein is executed to its developed phase: a streamlined system of surge model deployment that represents the spatial variability of Volusia County with consideration of elements such as cyclone track, wave action, and sea level rise, the results of which may be conveyed to pertinent social, governmental, and infrastructural institutions for informed decision making. FLAVOR is, in short, designed to pursue a resilient and sustainable future for coastal Volusia and Flagler Counties.

X. MESH DEVELOPMENT

The base HSOFS mesh used to produce FLAVOR was validated in 2015 by Riverside Technology Inc. & AECOM and is itself based on an earlier mesh created for the Extratropical Surge and Tide Operational Forecast System (ESTOFS). HSOFS is designed for computationally-efficient ensemble predictions across a large domain, hence its designation as an "on-demand forecast system." Efficiency is achieved by maintaining an average coastal resolution of 500 m, with its finest areas achieving a 150 m resolution. There are approximately 1.8 million nodes and 3.6 million elements in the HSOFS mesh (Riverside Technology Inc. & AECOM, 2015). The mesh is bounded by a smoothed 10 m inland elevation contour, implemented as a no flow boundary, and extends into rivers that are useful for coupled riverine-coastal modeling or terminates where inlet channel widths are reduced below 1,500 m. The St. John's River, a major riverine system running from its southern headwaters in Blue Cypress Lake to its northern outlet in Mayport along the East Coast of Florida just north of Jacksonville, is represented in its entirety. The Florida Everglades are largely unrepresented within HSOFS due to the complexity of its hydraulic features, but effects of this omission are unlikely to impact model results in northeast Florida.

In support of the research objective to produce a research-grade (i.e., high resolution) mesh for the Volusia County coast, HSOFS was chosen as the base mesh due to its extensive validation and low resolution, the latter of which provides computational efficiency outside of the area to be refined. Previous research by Thomas *et al.* (2022) affirms the claim that higher resolution translates to model accuracy; their research produced a US East Coast mesh called SAB (South Atlantic Bight) of 100 m average resolution and 20 m high-resolution in select areas. Resolution of this grade more accurately represents coastal topobathymetry; for example, the Port St. Lucie Inlet is represented by HSOFS as having width of 640 m and a center depth of 1.3 m, while the

SAB's fine resolution more accurately represents the inlet as having a width of 500 m and a center depth of 2.7 m. The mesh produced here represents Volusia County's coast to a resolution of 50 m, selected with the intention of providing an improvement over the SAB's model results and in order to capture a sufficient number of elevations across each coastal profile as illustrated in Figure 4.

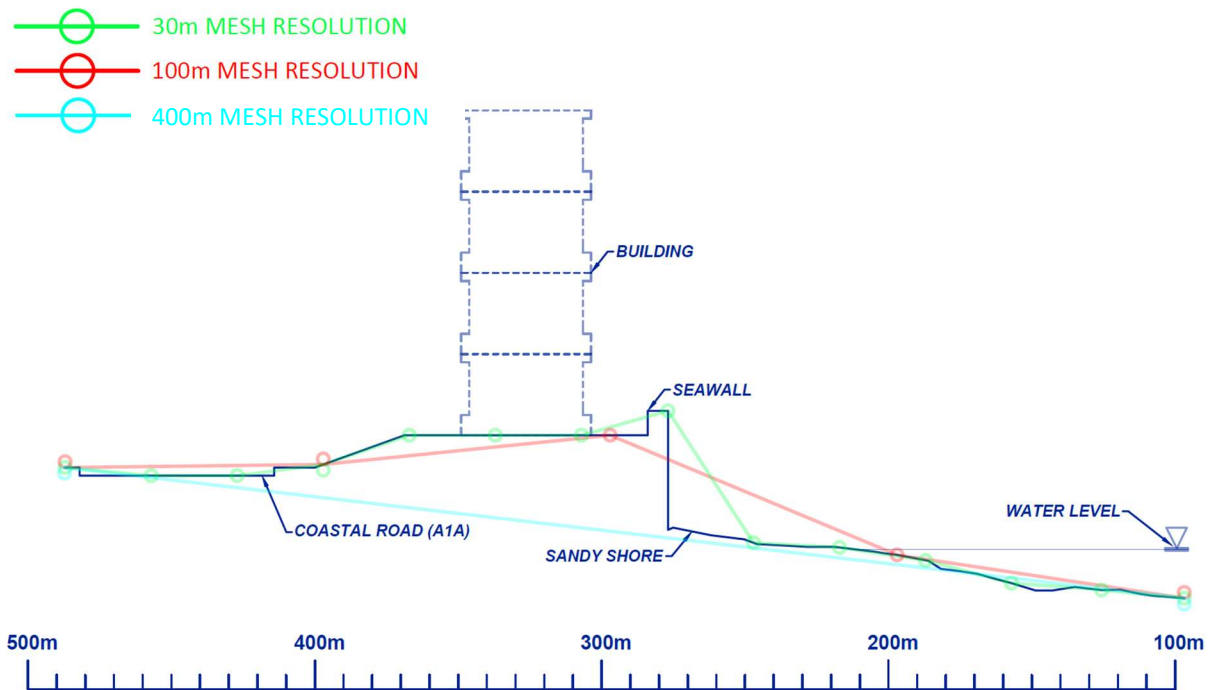


Figure 4 demonstrates the benefit of increased mesh resolution as a beach profile. From the ocean (right) to the land (left), it can be observed that an increased resolution, similar to that implemented in FLAVOR, can provide up to 10 times more elevation points for inundation to be more accurately simulated across. Fine resolution particularly represents vertical seawalls with a steeper, more accurate gradient than that modeled with a coarse resolution.

Surface-water Modeling System (SMS), a software package for surface-water modeling applications such as ADCIRC, provides tools for creating and editing meshes. Within SMS, 3 variants of the revised mesh, called FLAVOR, were created to explore the model outputs of several domains of HSOFS revision. Domains attempted include a large domain stretching from Cape Canaveral (28.27 degrees N) to north of Jacksonville (30.51 degrees N) and a small domain stretching from the Ponce De Leon Inlet (28.99 degrees N) to the Volusia/Flagler County line (29.37 degrees N). The former domain (large) was created to represent a vast coastal swath

centered around Volusia County's coast; this approach re-paved mesh elements to a low resolution in areas north and south of Volusia County which previously were of high resolution due to the fact that only Volusia County seawall feature lines were specified to have a 50 m node spacing. The latter domain (small) was created to mitigate this by producing high resolution within Volusia County but maintaining the carefully designed resolutions of areas outside Volusia County. Domains were created by delineating nodestring polygons with the aforementioned geographic spans and removing all existing HSOFS nodes within these areas. Each mesh variant contained a feature line drawn in ArcMap which precisely delineated the shape of Volusia County's seawalls before the hurricane season of 2022. Node spacing was forced to a specified interval of approximately 50 m along this feature line. Using this central seawall feature, a mesh was created from the nodes of 50 m spacing out to the boundary of the HSOFS cutout. The mesh type was set to utilize the "Paving (triangles)" scheme, which paves triangles from the feature line to the cutout boundary in this case or other feature lines more generally. Bias, which dictates how gradually mesh resolution changes as the mesh is paved, was set to 0.5, as this provided a balance between computational efficiency and resolution while maintaining the specified 30 m resolution along the seawall boundary. Other paving methods include Scalar Paving Density, which incorporates a size function to specify the geographic variability of how the modeler wishes to regulate resolution gradient from feature lines to cutout boundaries. Mesh element pavement was idealized for numerical stability using the nicegrid2 program produced by Fortunato *et al.* (2011). Boundary conditions of the base HSOFS mesh were maintained and renumbered to fit the FLAVOR mesh. Future variation of FLAVOR will specify different topobathymetric models: for example, one mesh variant could specify elevations interpolated from a 2018 (pre-Ian and Nicole) DEM, and another could specify elevations interpolated from a 2022 (post-Ian and Nicole) DEM.

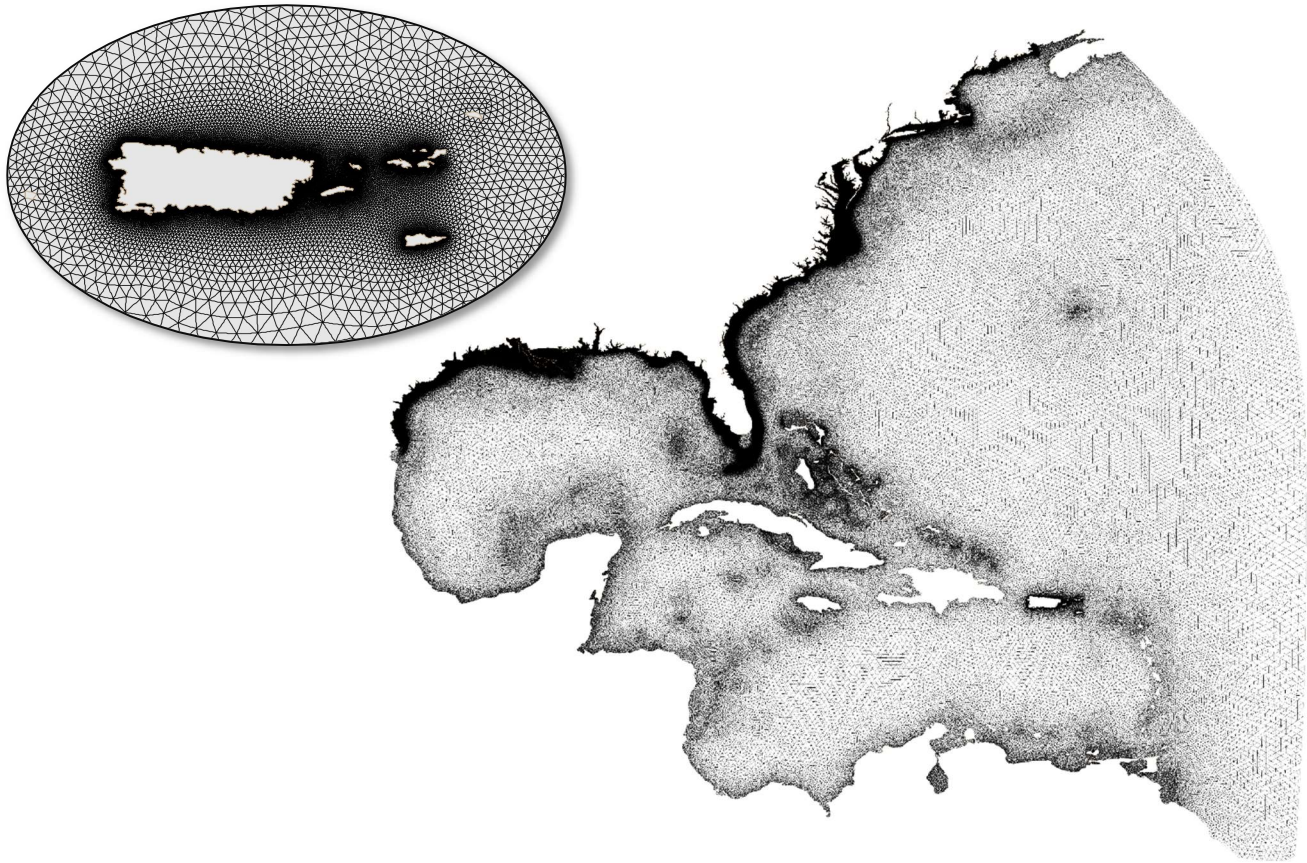


Figure 5 displays the HSOFS mesh in its full domain, stretching from the 65-degree W meridian (right) to the east coast of North and South Americas. Puerto Rico is enlarged (left) for detail; note the triangular mesh elements that vary in proportion and size in order to represent the spatial variability of coastal features.

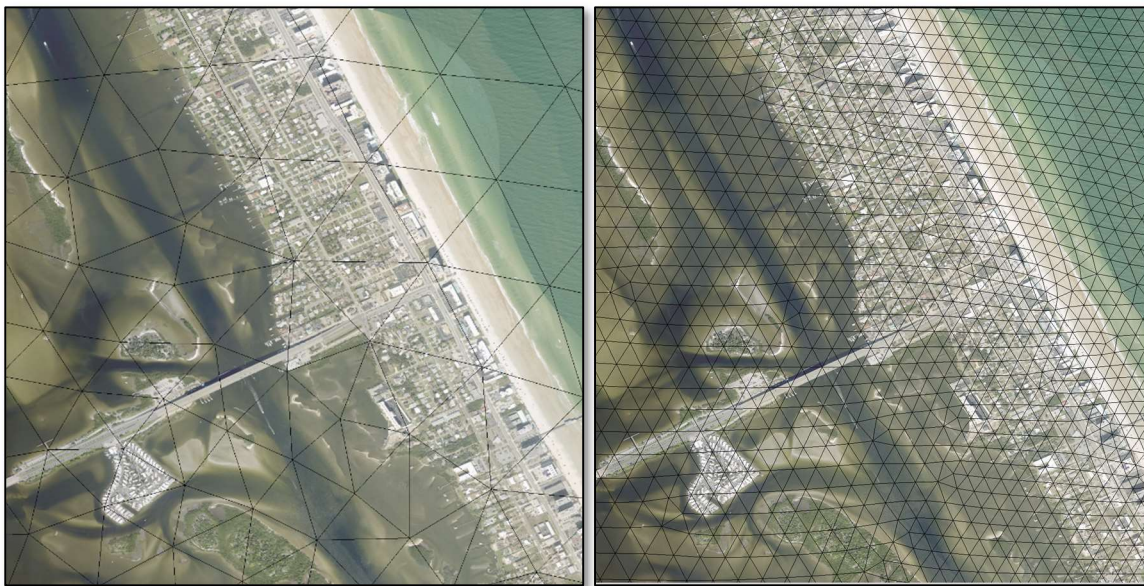


Figure 6 displays the HSOFS mesh (left) and the FLAVOR mesh (right) overlaid atop an aerial of Daytona Beach. The HSOFS resolution is 300 to 400 m in this area, while FLAVOR provides a resolution of approximately 50 m along the seawall.

XI. MODEL DEVELOPMENT

The FLAVOR model was developed incrementally to facilitate performance evaluation at each step. The first increment included model runs with only tidal inputs. ADCIRC tidal constituents are parameterized as harmonic waves that propagate from the open ocean boundary of an unstructured mesh; each constituent represents the tidal fluctuation of water surface elevation resulting from a variety of sources, most of which represent astronomical influences. The graphs of these show oscillations which vary in amplitude as time varies; Figure 7 is an example of this.

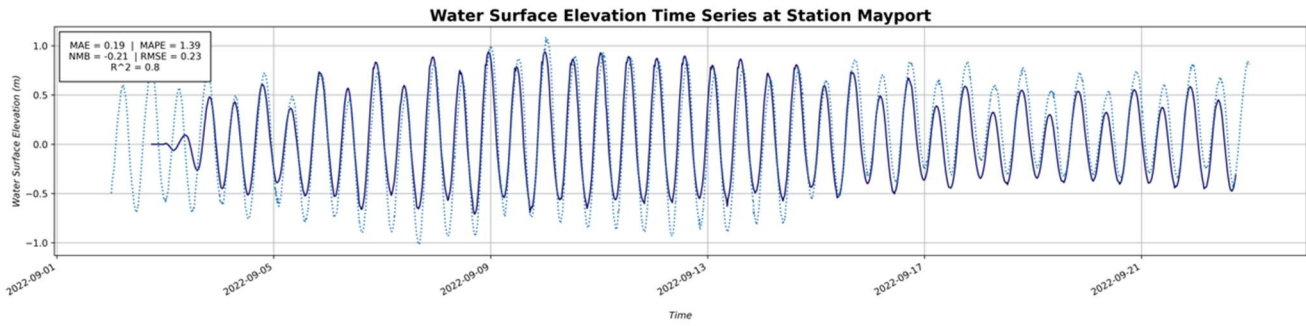


Figure 7 demonstrates the oscillatory pattern of water surface elevation across a FLAVOR model run with only tidal forcings. These oscillations are shown atop observations provided by NOAA from the tidal station located in Mayport, FL. Note the spring tide, in which tidal variations are large, and the neap tide, in which tidal variations are moderate.

This pattern of oscillation repeats at a set interval, called an epoch, depending on the tidal constituent. For example, the moon, denoted as the “M2” or “principal lunar semidiurnal” tidal constituent, exerts tidal influence in a spatially varying manner across the earth’s surface and is dependent on the moon’s alignment and proximity to the earth; every 28 days, this oscillatory cycle describing the moon’s influence repeats, therefore defining a lunar epoch to be 28 days. All 37 harmonics may be used to describe tidal fluctuations within the ADCIRC model (many of which exert negligible influence on the earth’s tidal water bodies), and the synthesized harmonic of these constitutes an approximately 18-year epoch (National Oceanic and Atmospheric Administration). The spatial variation of harmonic constituents are globally defined by running extended ADCIRC

simulations and are updated periodically; these model results are referred to as the “ADCIRC tidal database.” Using the ADCIRC2015 tidal database (Szpilka *et al.*, 2016), the 8 primary tidal constituents outlined in Table 5 were applied; these 8 were chosen out of the 37 total because they constitute the majority of the tidal forcing amplitude (in other words, minimal accuracy is added by incorporating the remaining 29); this is a common approach in the ADCIRC literature. This database was most recently updated in 2015 and was produced with updated bathymetry, open ocean boundary placement, refined bottom friction data, incorporation of advective terms (which enhances output within certain estuaries and tidally influenced rivers), boundary forcing, and coastal resolution. Of these improvements, the bathymetry and resolution enhancements are attributed to improvement in the M2 constituent, the primary lunar constituent. The authors of the database noted that ambiguity exists within the ADCIRC2015 database regarding bottom friction of inland bodies, which may impact the performance of tidal constituents within the marshy coastline of this research's Floridian coastline.

In the model control file, tidal constituents are specified first using brief, generalized parameters according to constituent, then a lengthy segment of the file defines each constituent in terms of individual boundary forcing nodes. Within the former section, nodal factor and equilibrium argument, represented by the parameters $FF(T)$ and $FACE(T)$, are calculated based on simulation timing within the Fortran program `tide_fac.f`, which is available under the "ADCIRC Utility Programs" page of adcirc.org.

Table 5 summarizes the 8 primary tidal constituents used to force the FLAVOR model in both the tides-only incremental validation as well as the meteorologically forced final variation.

CONSTITUENT NAME	CONSTITUENT DESCRIPTION
K1	Lunisolar declinational diurnal
K2	Lunisolar semidiurnal
M2	Principal lunar semidiurnal
N2	
O1	Principal lunar declinational diurnal
P1	Principal solar declinational diurnal
Q1	
S2	Principal solar semidiurnal

At this stage, no meteorological forcing was incorporated to assess the integrity of the model's fundamental tidal simulation. Initial model runs were identical to those specified in HSOFS development (2015), except for the timing, which was set to span 25 days following September 11th (an interval containing Ian, which made landfall September 29th) for the first run and to span 25 days following October 24th (an interval containing Nicole, which made landfall November 10th) for the second run. Metrics of agreement were developed to assess model performance and are outlined in the following section; these metrics were assessed and adjustments were made to model inputs where necessary. ADCIRC inputs are outlined below:

Bottom friction is represented by the parameter NOLIBF and was set to 1, prompting ADCIRC to use the quadratic bottom friction law in reference to the Manning's n nodal attribute specified in the original HSOFS mesh.

Coriolis behavior is represented by the parameter NCOR and was set to 1, prompting ADCIRC to employ a variable Coriolis effect about a center longitude of -71 (SLAM0) and center latitude of 27 (SFEA0) specified in the original HSOFS mesh.

Minimum angle for tangential flow is represented by the parameter ANGINN and was set to 110.

Model type is represented by the parameter IM and was set to 0, prompting ADCIRC to run a 2-dimensional depth integrated (2DDI) barotropic model using the generalized wave continuity equations (GWCE) and momentum equation formulations.

Finite amplitude terms are represented by the parameter NOLIFA and were set to 2, prompting ADCIRC to employ wetting and drying algorithms, interpret bathymetric depths as specified in the fort.14 grid file to represent initial water depths, and include finite amplitude terms in the model run. Minimum depth was specified as 0.05 m.

TAU0, which represents the Generalized Wave Continuity Equation (GWCE) weighting factor, was set to -3, prompting ADCIRC to vary this parameter in relation to both space and time. This variation in TAU0 is dependent on the TAU0Base parameter within the fort.13 nodal attribute file, which is itself dependent on depth and distance between nodes. The nodal attribute "primitive_weighting_in_continuity_equation" is specified in the model parameter and periodic boundary condition file (fort.15), so the TAU0 attribute is ignored.

Time step (seconds) and **length of run** (days) were represented by the parameters DTDP and RNDAY and were set to 2.0 and 28.5, respectively, denoting a 28.5 day simulation time (that is, the simulation *represents* 28.5 days but does not take that long to run) with calculations performed every 2 seconds across the domain.

General ramp period was represented by the parameter DRAMP and was set to equal 5.0 days, prompting ADCIRC to gradually "ramp up" model forcing over a 5-day simulation period. The number of hyperbolic tangent spin up ramps, denoted by the parameter NRAMP, was consequently set to 1.

Meteorological forcing represented by the parameter NWS was set to 0 for the tides only runs to omit meteorological forcing. For the Hurricane Ian simulations, NWS was set to 20, prompting ADCIRC to use the data from the National Hurricane Center Best-Track files, converted to ADCIRC fort.22 files, to produce time-varying distribution of hurricane winds and pressures using an internal Generalized Asymmetric Holland Model (adcirc.org).

Total model **run time** of 28.5 days is comprised of a 5 day ramp up period, a 3-day dynamic steady state period allowing for stabilization of the model prior to the true simulation period, a fully-forced and stabilized period of 16.5 days, and an output period of 4 days. Hurricane landfall for Volusia County was intended to take place on day 26.5 of the total model period, allowing 2 days of model output prior and following. In the case of Hurricane Ian, the 28.5-day timeline spanned from September 2nd at 12:00 PM (noon) to October 1st at 12:00 AM (midnight). Model output time was set to begin September 27th at 12:00 AM (midnight) and to end on October 1st at 12:00 AM (midnight).

XII. MESH & MODEL VALIDATION

Surge water level observations were gathered from recording stations, the data of which was made available by NOAA and the US Geological Survey (USGS). NOAA provides both tidal predictions and tidal observations from permanently fixed stations along the coastline and within some tidally influenced inland bodies on their Tides and Currents website. USGS provides flow observations from permanently fixed riverine stations and rapidly deploys temporary coastal recording stations in the event of significant coastal storm events; furthermore, USGS performs post-storm assessments for major hurricanes and provides surveyed high-water mark data that is regarded among coastal modeling literature as legitimate data for model validation (Bilksie, Coggin, Hagen, and Medeiros, 2015; Thomas, Dietrich, Dawson, and Luettich, 2022). NOAA's data is constantly recorded and extensively validated; due to the temporary deployments of USGS stations as well as the fact that some storms, including Nicole, were not recorded by USGS, NOAA's data was identified as the primary source for model validation. The placement of the nearest recording stations on Trident Pier (Cape Canaveral, FL, 100 km south of Daytona Beach) and the Mayport Naval Station (Mayport Florida, terminal end of St. John's River into Atlantic Ocean, 150 km north of Daytona Beach) well outside of FLAVOR's domain means that FLAVOR's local performance will not be well represented at these locations. It is therefore necessary to further validate FLAVOR's performance using the *in-situ* USGS data where possible. It should be noted that NOAA provides tidal predictions for Daytona Beach using computer software, but no *in-situ* data is recorded. In addition to NOAA and USGS data, photographic documentation of Volusia County's coast following Hurricanes Ian and Nicole provide a means of qualitatively verifying surge elevation and velocity output using scientific intuition.



Figure 8 contextualizes the 5 NOAA stations used for model validation in relation to the Volusia County coastline of interest (yellow polygon).

These data sources were assembled using Python, and time series plots were produced for NOAA tide predictions, NOAA/NOS tide observations, and FLAVOR tide predictions. The NOAA and FLAVOR predictions were first evaluated in the tides-only stage of model development, and all sources were used to validate the FLAVOR model with meteorological forcing. The quantitative process is identical in both scenarios and is outlined here, and NOAA/NOS data will be referred to as "observed data." Visual validation was performed by superimposing FLAVOR predictions onto observed data; particular attention was paid to the congruency of tidal oscillations, the amplitude of individual oscillations, and the trend of neap and spring tides over the course of a lunar cycle. Previous studies are especially concerned with the equality of predicted and observed peaks, and it is common for predicted troughs to register at higher water levels than observed; this is of little concern, as it is the peaks of tidal fluctuations that result in maximized damage. Moreover, the addition of meteorological forcing is likely to dominate surge behavior in the event of a tropical cyclone, and these tidal discrepancies are not significant.

XIII. RESULTS

Elevation

Across the HSOFS domain, the FLAVOR mesh produced comparable results to those of HSOFS for hurricanes Ian and Nicole. Minor variations were evident at NOAA recording stations outside the FLAVOR domain of refinement. Variations were on the order of 0.01 m for mean absolute error (MAE) and mean absolute percentage error (MAPE) and were likely a result of different elevation and velocity propagations stemming from the area of refinement. FLAVOR modeled maximum depths (relative to NAVD88) ranged from -3.42 m in the deep ocean to 9.84 m on land, and HSOFS modeled maximum depths ranged from -3.41 m in the deep ocean to 9.83 m on land.

NOAA Tidal Station Time Series Analysis

Localized validation for the Volusia County oriented FLAVOR mesh was accomplished using 3 primary data sources: permanent NOAA tidal gauges, fixed across Florida's coast but outside the domain of the HSOFS revised area within FLAVOR, temporary coastal and riverine gages deployed by USGS in the event of a tropical cyclone, and high-water marks (HWM) surveyed following landfall of a tropical cyclone. The first of these sources was evaluated using time series representing water elevation throughout the model period, and the maximum elevations from all sources were compiled into a sample group on which linear regression was performed. For a tides-only simulation of Hurricane Ian, which spanned a 19-day period leading up to the start of the meteorological simulation, FLAVOR modeled surge elevations with an average R^2 value of 0.796 relative to 5 permanent NOAA tidal stations throughout Florida's east coast, while HSOFS produced surge elevations with an average R^2 value of 0.798 relative to these same stations.

HSOFS better models peak values, which rarely result in errors greater than 0.1 m on the coast, while trough values modeled by HSOFS tend to overpredict up to 0.25 m. The same contrast between peak and trough errors stands true for FLAVOR. HSOFS tidal oscillations were uniform and displayed only two instances of 2-4 hour phase lag for the Fernandina Beach and Mayport (coastal NE Florida) tide stations from simulation time spanning 09/27/2022 to 10/01/2022, as was the case for FLAVOR. RMSE was, on average, 0.198 for all time values within FLAVOR and HSOFS time series; each tidal station output documents identical RMSE for FLAVOR and HSOFS tidal runs.

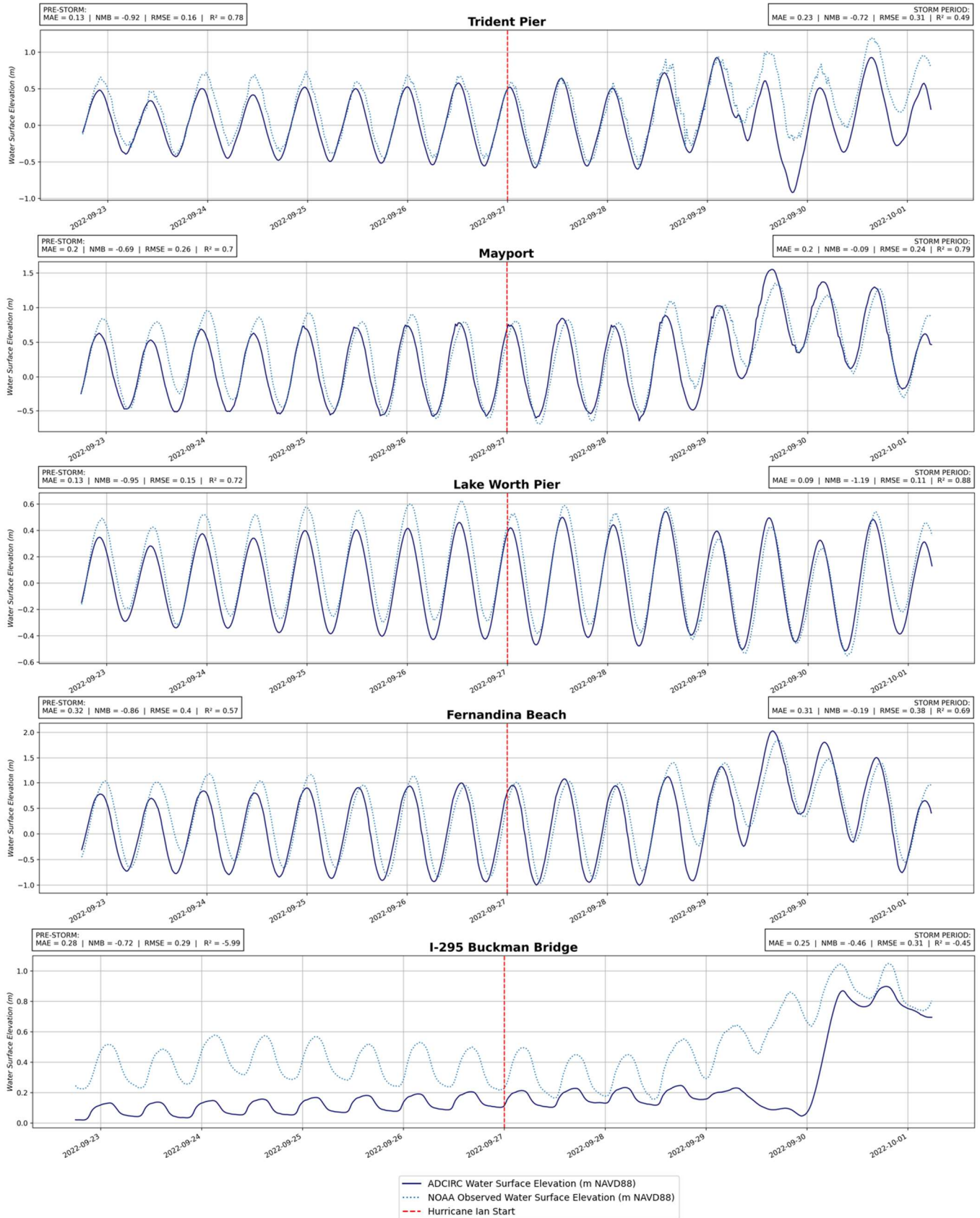


Figure 9 demonstrates FLAVOR agreement with observed data recorded at 5 NOAA Tides and Currents stations for a meteorological simulation of Hurricane Ian. The first 4 of these are located coastally, while the I-295 Buckman Bridge station is located on an inland, tidally influenced body; the FLAVOR model shows comparable results to the previously validated HSOFS model.

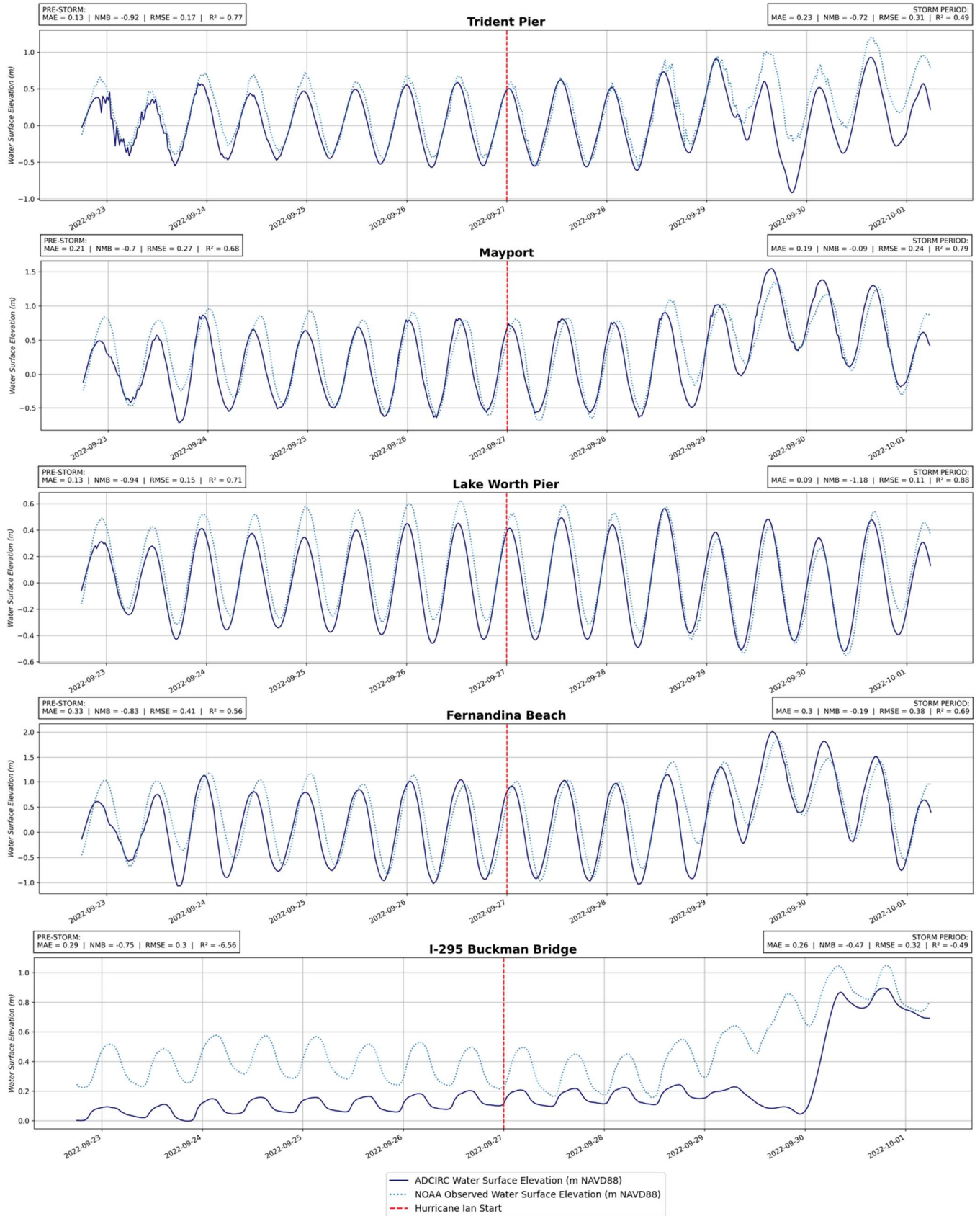


Figure 10 demonstrates HSOFS agreement with observed data recorded at 5 NOAA Tides and Currents stations for a meteorological simulation of Hurricane Ian. The first 4 of these are located coastally, while the I-295 Buckman Bridge station is located on an inland, tidally influenced body. Note the y-axis scaling and the error metrics listed in the upper left corner.

Table 6 compares HSOFS and FLAVOR elevation results to true elevation. Elevation data within the FLAVOR domain was difficult to obtain and predominantly unconsidered in this chart. Stations colored red in the “Vicinity” column are outside the boundaries of Volusia County, while stations colored green are located inside the boundaries of Volusia County.

STATION	TYPE	VICINITY	FLAVOR PREDICTED (m)	HSOFS PREDICTED (m)	OBSERVED (m)	FLAVOR DISCREPANCY (m)	HSOFS DISCREPANCY (m)
BUCKMAN BRIDGE	NOAA TIDAL STATION	OUTSIDE VOLUSIA COUNTY	0.898	0.896526	1.0381665	-0.140	-0.142
FERNANDINA BEACH	NOAA TIDAL STATION	OUTSIDE VOLUSIA COUNTY	2.029	2.012	1.728667	0.301	0.283
HALIFAX RIVER	USGS TIDAL STATION	INSIDE VOLUSIA COUNTY	0.567	0.681	1.152	-0.585	-0.471
LAKE WORTH PIER	NOAA TIDAL STATION	OUTSIDE VOLUSIA COUNTY	0.544	0.564	0.595	-0.051	-0.031
MAYPORT	NOAA TIDAL STATION	OUTSIDE VOLUSIA COUNTY	1.551	1.546	1.274667	0.276	0.271
NEW SMYRNA BEACH PIER	HIGH WATER MARK	INSIDE VOLUSIA COUNTY	1.334	1.022	0.247	1.087	0.775
PONCE INLET	HIGH WATER MARK	INSIDE VOLUSIA COUNTY	1.721	1.664	2.256	-0.535	-0.592
PONCE INLET	VIRTUAL TIDAL STATION	INSIDE VOLUSIA COUNTY	1.524	1.467	2.243	-0.719	-0.776
SUNGLOW PIER	USGS RAPIDLY DEPLOYABLE GAGE	INSIDE VOLUSIA COUNTY	1.726	1.709	2.25	-0.524	-0.541
TRIDENT PIER	NOAA TIDAL STATION	OUTSIDE VOLUSIA COUNTY	0.972	0.930	1.196667	-0.224	-0.266

FLAVOR RMSE (m)	HSOFS RMSE (m)
0.53	0.48

Peak Value Analysis

As a second investigation into the sufficiency of the FLAVOR model within its region of application, flood depths were verified using high water marks from USGS post-storm surveys as well as the riverine and coastal gages; some of these gages are permanently fixed, while others are rapidly deployed in the event of a tropical cyclone. A challenge of this analysis is the scarcity of data available in Volusia County; where more populous counties are data rich, Volusia County was

not prioritized in post-cyclone data collection, and where there are data descriptive of Volusia County post-cyclone conditions, its geographic point of collection was rarely near the seawall feature line along which FLAVOR was refined. In total, 3 points of collection lie within areas where FLAVOR resolution is approximately 50 m. Locations outside of FLAVOR and HSOFS results were not considered in this assessment. Together, these data sources provided 10 samples of high-water elevation. The results presented in Table 6 are limited to concluding only general high-water agreement across Florida's east coast; the values presented here provide no insight regarding surface water elevation of surge throughout Hurricane Ian's duration, and conclusions are moreover limited by the ambiguity of High-Water Mark (HWM) metrics, which are measured from ambiguous bands of debris or water stains as shown in Figure 11. HWM's are therefore regarded as only marginally reliable for model validation in this research.



Figure 11 shows a Florida Department of Environmental Protection (2022) employee indicating the approximate height of a stain line left by Hurricane Ian in Naples, FL. Note the roughly 1/2 foot width of the stain line; this broadness results in ambiguity of measurement, and High Water Marks are therefore regarded as only marginally reliable for validation purposes.

Velocity

To analyze velocity data across a small sample size (i.e., coastal ADCIRC output only at HSOFS and FLAVOR nodes) exhibiting non-Gaussian form, the bootstrapping method was employed; the methodology is described below.

Bootstrapping

For small sample sizes or samples which exhibit non-Gaussian form when plotted as a histogram, bootstrapping is a method of producing a large number of virtual samples created from the original sample set. Though not true in all cases, the histogram created by plotting the bootstrapped means (or other statistical measures) tends to appear roughly Gaussian; in this event, probabilistic methods may be employed to evaluate results. For increased data integrity, a bootstrapping operation, in which an acceptable sample size (generally taken to be 30) can be sampled thousands of times to produce a virtual sample size on the order of 10,000. A p-test may be performed to compare two such datasets, in which a test statistic (i.e., mean) of the analyzed data may be assessed in terms of the number of standard deviations it lies from the same test statistic of a validated dataset. The p-value that results from such a test may be analyzed to determine acceptance or rejection of a null hypothesis.

In the context of the discussed FLAVOR-HSOFS comparison, coastal velocity output for both models results in non-Gaussian histograms, and the bootstrapping methodology described above was employed to create virtual samples of sufficient size describing the maximum velocities produced by both models; here, the HSOFS maximum velocity dataset is regarded as the validated dataset to which the FLAVOR maximum velocity dataset is compared. That the chosen test statistic (mean) for FLAVOR is identical to that of HSOFS is the null hypothesis to be accepted or rejected.

The datasets for this procedure were derived by first identifying a boundary that encircled a line of HSOFS nodes roughly following the length of Volusia County’s barrier island as well as one additional node on the roughly east and west sides of the line; therefore, the boundary of analysis is approximately the span of 3 HSOFS nodes, or the width of 2 elements, and spans longitudinally from the Ponce de Leon inlet (south) to the Volusia/Flagler County line (north). The same boundary was used to select FLAVOR coastal nodes, and, given the enhanced resolution of the FLAVOR mesh, this boundary consequently encircled more FLAVOR nodes than HSOFS nodes; in total, 967 HSOFS nodes and 15,872 FLAVOR nodes were encircled by the boundary. All nodes which registered no surge velocities (i.e., dry nodes) were ignored during this operation. Maximum velocity output at each wetted node was extracted from the corresponding maxvel.63 file, and samples of size 967 were taken with replacement 10,000 times. The histograms describing surge velocity recorded across these nodes are displayed in Figure 12.

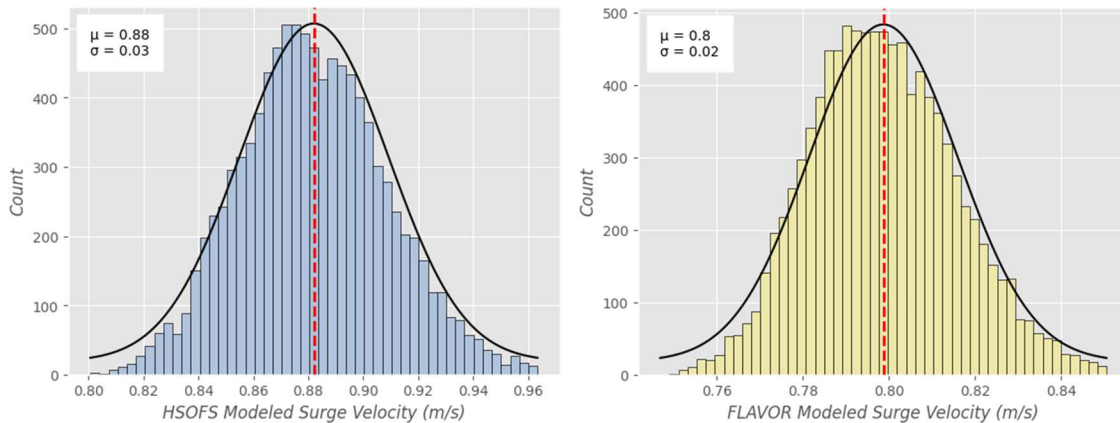


Figure 12 compares HSOFS and FLAVOR velocity results following the bootstrap operation performed on the non-Gaussian datasets. The operation confirms that FLAVOR mean coastal velocities lie outside 2 standard deviations of the HSOFS mean; more specifically, the FLAVOR mean coastal velocity of 0.8 m/s has a 0.39% probability of being sampled by chance (P -Value = 0.0039, $1-P = 0.9961$). Therefore, the velocity results of FLAVOR are statistically significant relative to HSOFS.

The results of this operation confirm the tendency of FLAVOR to produce lower velocity results than HSOFS. The latter of these produced a mean of 0.88 m/s and standard deviation of 0.03 m/s; the former produced a mean of 0.80 m/s, which lies within 2.67 standard deviations of

the HSOFS mean. There is a 0.39% chance (P-Value = 0.0039, 1-P = 0.9961) of these bootstrap sample results occurring by chance, and this result is therefore confirmed as statistically significant. The null hypothesis can be rejected as in the following statement: it is not true that HSOFS and FLAVOR meshes produce identical velocity output within the coastal region of Volusia County. This conclusion is limited to those exact words, and no conclusion can be made regarding the superiority or inferiority of either model given the absence of observation data.

Visual Analysis

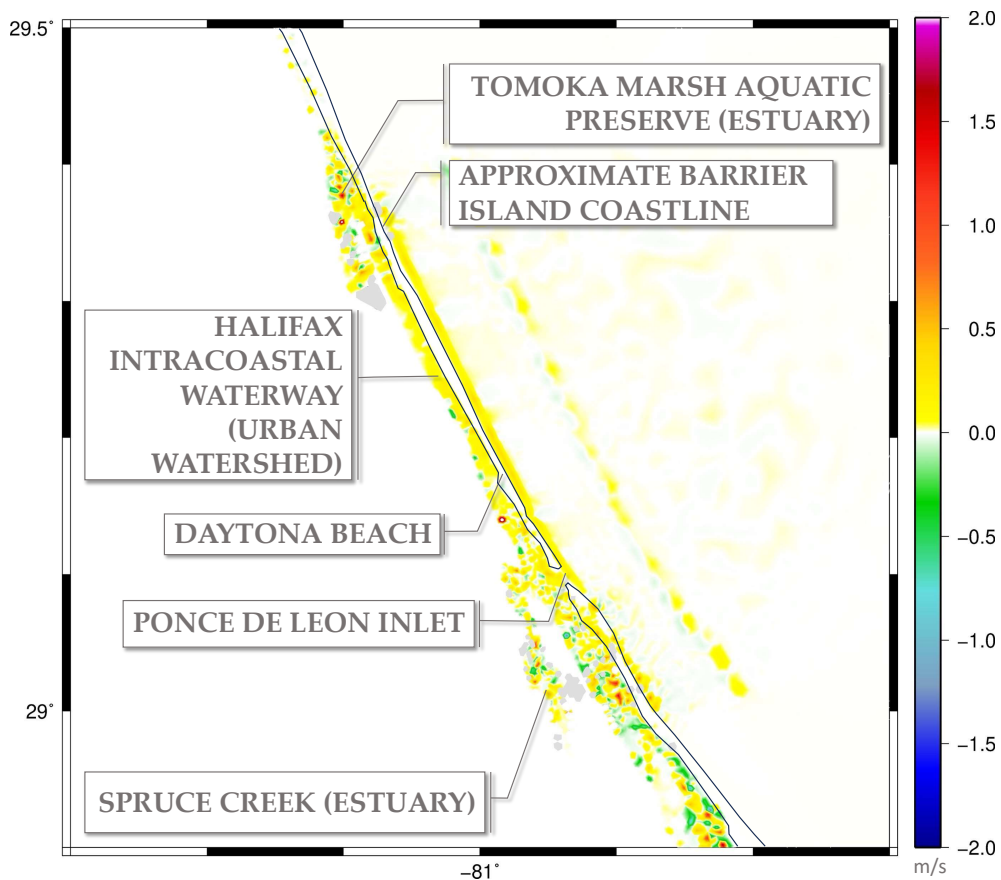


Figure 13 rasterizes velocity differences between HSOFS and FLAVOR output in the domain of refinement of FLAVOR. Significant differences occur in estuarine and tidal flat regions.

A comparison raster of FLAVOR velocity output subtracted from HSOFS velocity output is displayed in Figure 13. Velocities show few to no differences in open ocean but deviate from

each other nearshore. The entire domain of FLAVOR refinement, which spans the coastline from the southern tip of the northern peninsula of Volusia County to the Volusia/Flagler County line (north of the Tomoka Marsh Aquatic Preserve), contains velocity differences on the order of +/- 0.25 to +/- 0.5 m/s between HSOFS and FLAVOR output, and total velocity outputs produced by both are on the order of 1 m to 1.5 m. Along the seawall, differences peak to approximately 0.5 m/s but average around 0.3 m/s (positive), concluding that HSOFS seawall velocities are greater than those produced by FLAVOR; this is consistent with the bootstrapping results from Figure 12. These differences are exaggerated along the tidal flats and islands along the intracoastal waterway; FLAVOR's refined resolution provides more precise output in these areas of low elevation gradient, the inundation of which are not well represented by the large elements of HSOFS.

Note the areas of extreme differences (represented on a spectrum between red and magenta); in these regions, either HSOFS or FLAVOR (or both) likely yield instability, HSOFS in the direction of extreme positive velocities and/or FLAVOR in the direction of extreme negative velocities, which can be deduced by the fact that velocity differences in those locations are represented as positive and that they display a gradient from red around the outer perimeter of what appear to be mesh elements to white, representing that these differences approach an extreme that lies outside of the specified -2 to +2 m/s range of display. Also note the gray patches along the tips of estuarine boundaries; these imply differences in inundation extent between HSOFS and FLAVOR, a result expected from the outset of this research. As in the case of the research presented by Thomas *et al.* (2022), this increased inundation extent predicted by FLAVOR positions the refined model to be more seamlessly incorporated into hydraulic models of inland conveyance.

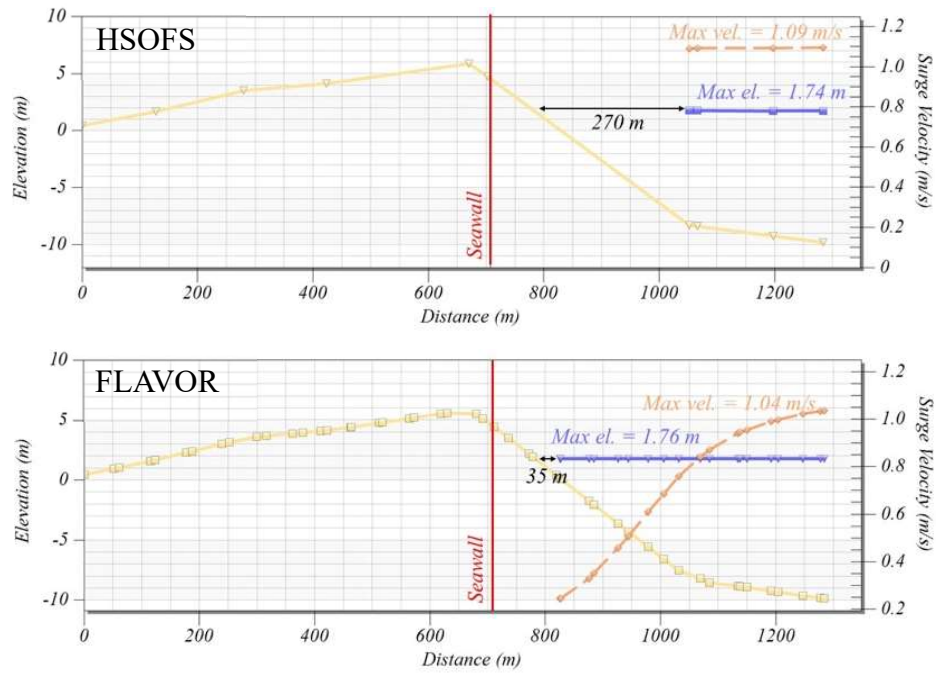
Investigating model output by charting beach profiles is a novel approach to understanding model performance, and it is particularly useful for spatial comparison of output between the

HSOFS and the FLAVOR models. This methodology consists of plotting surface water elevation, surge velocity, and topography of a single latitudinal length and was employed at 10 locations where citizen photos, the authors of which remain anonymous by request, were taken and submitted to ERAU. Figure 14 maps these locations and delineates the 1,000 m wide feature lines across which profiles were created. Locations represent a range of infrastructure, including home residential (i.e., Wilbur-By-The-Sea), condominium residential (i.e., St. Kitts Condo), commercial (i.e., 7/11 gas station), and public (i.e., Frank Rendon Park). This thesis describes the profiles taken at Wilbur-By-The-Sea and Frank Rendon Park, and the remaining 8 are included as figures.



Figure 14 represents the 10 locations at which citizen photographs were taken and submitted anonymously to ERAU. Locations represent a range of infrastructural purposes, such as high-density residential (i.e., condominiums) to public spaces (i.e., beach-front parking and recreation). The latitudinal lines represent the 1,000 m spans of 10 beach profiles created to visually compare HSOFS and FLAVOR; these observations can be seen on the following pages.

Frank Rendon Park is a parking lot and public facility located on the coast of Daytona Beach Shores. The facility sustained damage to its pavement resulting from washout of underlying sand as well as minor damage to its seawall. Surge model output provides insight regarding the elevation and velocity of seawater impacting the facility during Hurricane Ian, and the maximum values of these outputs as well as photographic documentation of Frank Rendon Park can be observed in Figure 15. Note the finer node spacing of FLAVOR output and input compared to HSOFS; this effect is what was predicted in Figure 4 to occur following mesh refinement. Resulting from this refinement, FLAVOR inundation extent is more representative than HSOFS of the fact that Frank Rendon Park's eastern edge was impacted by surge, as evinced by the non-existence of HSOFS surge data leftward of 1,000 m and the extension of FLAVOR surge data as far as the 800 m gridline, which is closer to the vertical red line representative of the seawall at that location; the remaining disparity between observed damage and FLAVOR's modeled gap between seawall and surge extent can be addressed with further refinement and incorporation of a wave model. Note the trend of surge velocity upon seawall approach. HSOFS models surge to vary within only 0.004 m/s of 1.09 m/s; leftward of the 1,000 m gridline, no velocity is modeled. FLAVOR models surge as gradually reducing from 1.04 m/s to 0.24 m/s as it propagates westward. Though surge is not modeled as reaching the seawall, this gradual declination provides a more precise value of surge velocity upon contact with the seawall.



— MAXIMUM SURGE VELOCITY
— MAXIMUM SURFACE WATER ELEVATION
— TOPOGRAPHIC GRADIENT

Figure 15 illustrates surge extent, elevation, and velocity upon approach towards the seawall at Frank Rendon Park, a public facility with parking and playground amenities. Note the finer resolution of FLAVOR output and input as well as the greater surge extent modeled by FLAVOR. This information is regarded as providing more precise detail in terms of evaluation surge velocity and elevation upon impact with the seawall.

Wilbur-By-The-Sea is a coastal neighborhood of Volusia County that made national headlines following Hurricane Nicole, which caused several homes in Wilbur-By-The-Sea to collapse into the ocean due to seawall and dune washout. Figure 16 demonstrates the maximum recorded surface water elevation and velocity of the surge induced by Hurricane Ian as modeled by FLAVOR and HSOFS at a home in this community. Note the water surface elevation representative of the intracoastal waterway (Halifax River) extending from gridline 0 m to 100 m. Profiles across all 10 locations, including Frank Rendon Park and Wilbur-By-The-Sea, are available on the following 2 pages.

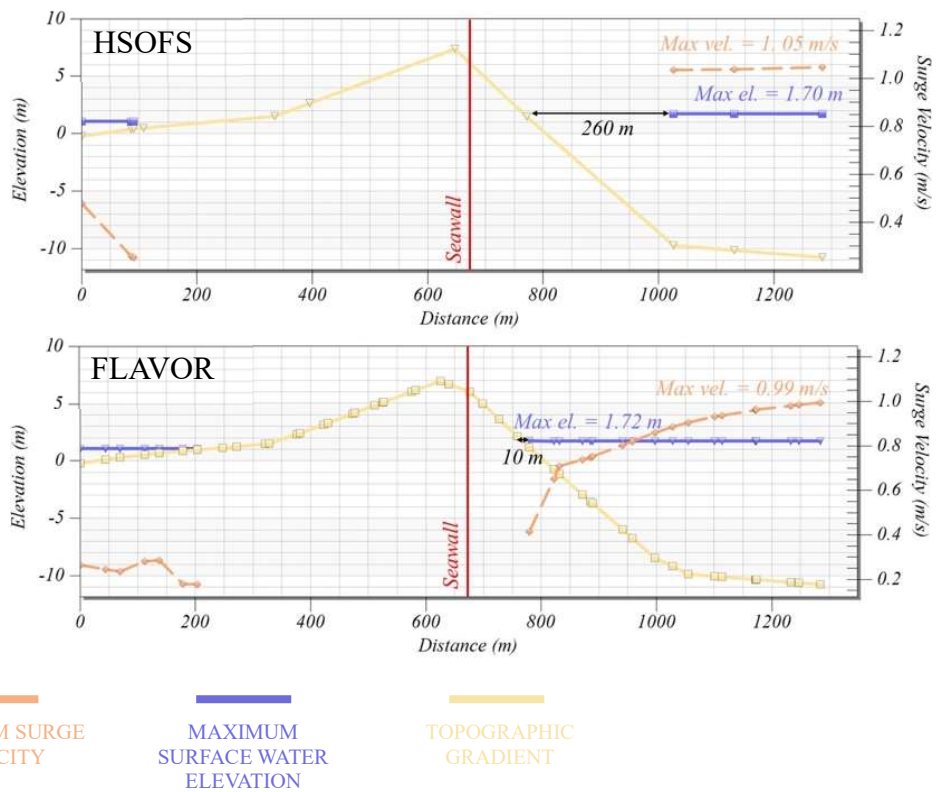
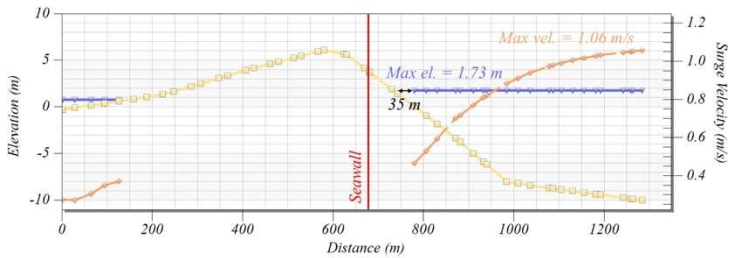
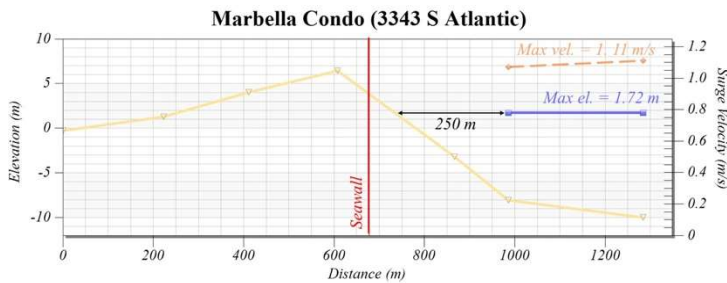
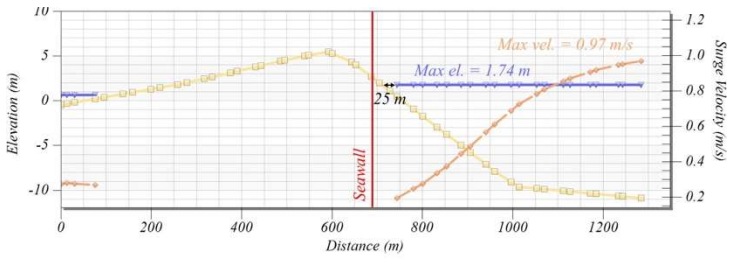
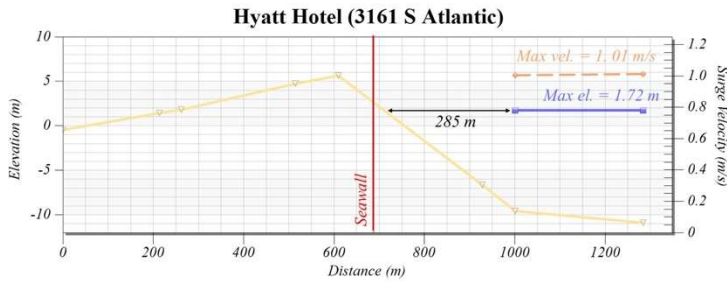
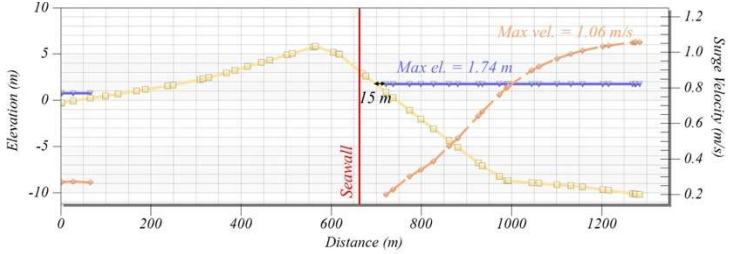
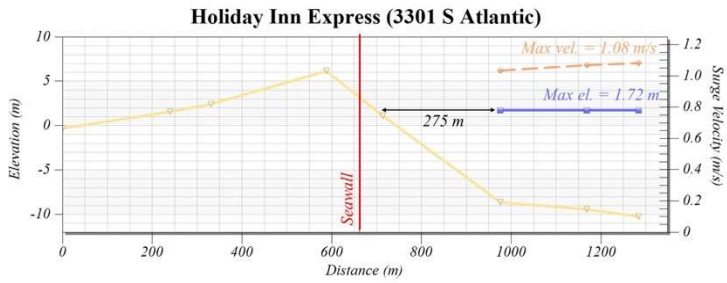
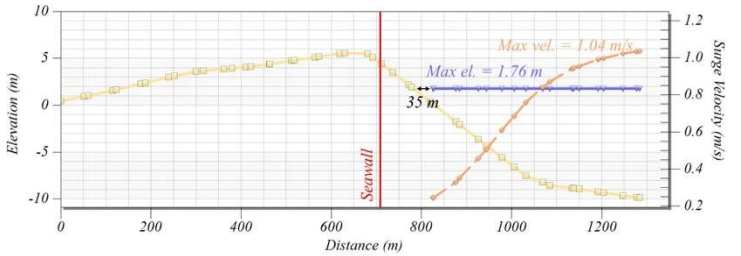
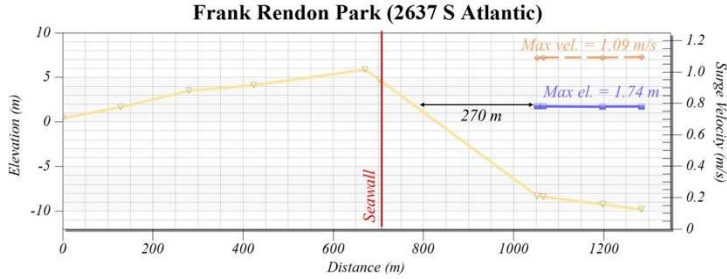
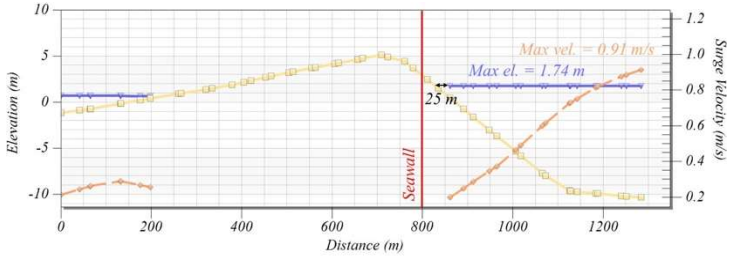
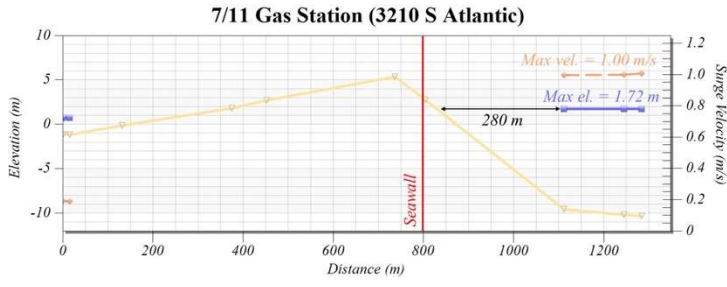


Figure 16 illustrates surge extent, elevation, and velocity upon approach towards a home in Wilbur-By-The-Sea, a residential area made famous for the homes that collapsed into the Atlantic following hurricane Nicole. Note the finer resolution of FLAVOR output and input as well as the greater surge extent modeled by FLAVOR. This information is regarded as providing more precise detail in terms of evaluation surge velocity and elevation upon impact with the seawall. Also note the intracoastal waterway on the left of the profile.

HSOFS

FLAVOR



— MAXIMUM SURGE VELOCITY
— MAXIMUM SURFACE WATER ELEVATION
— TOPOGRAPHIC GRADIENT

HSOFS

FLAVOR

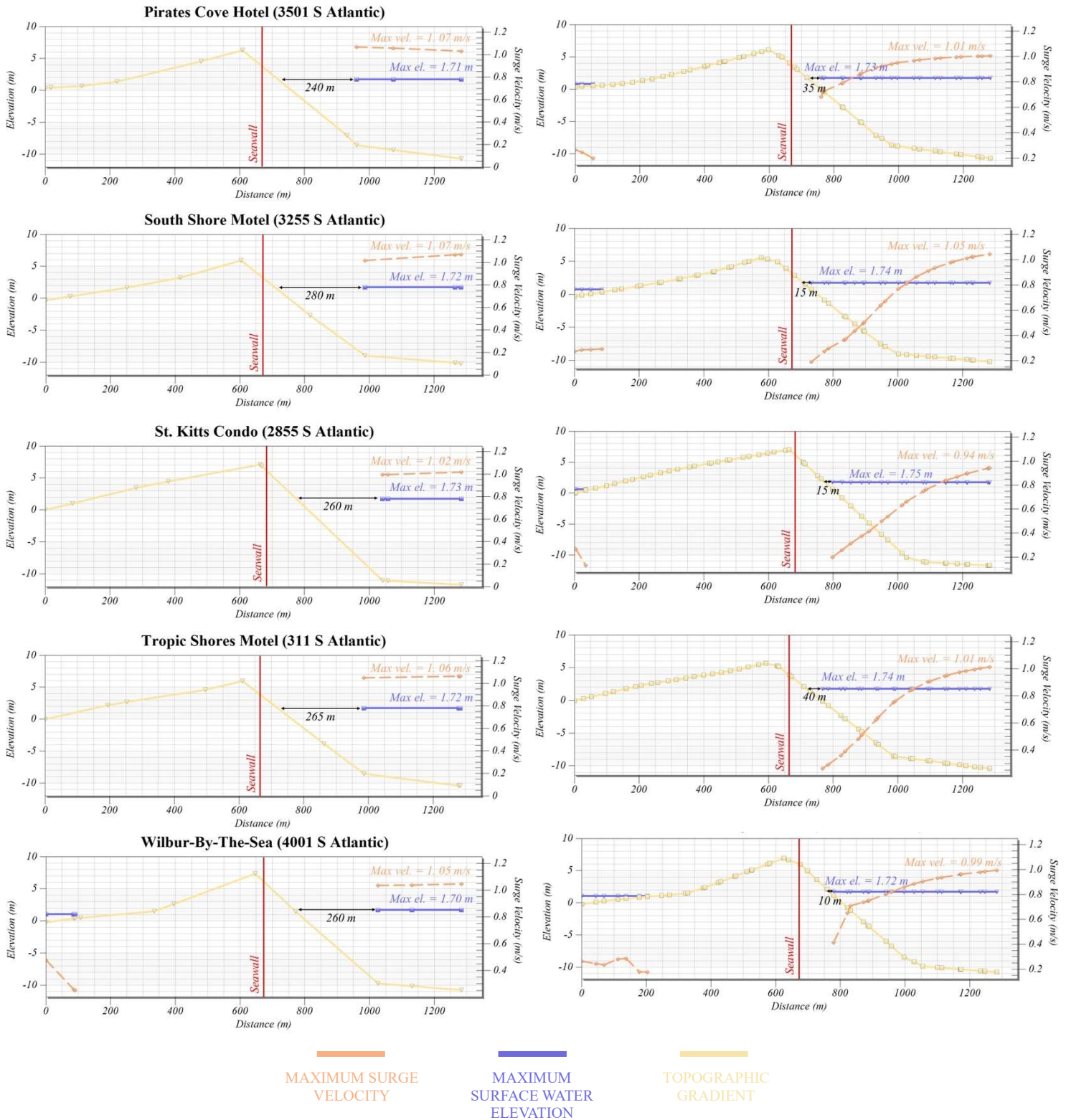


Figure 17 illustrates surge extent, elevation, and velocity upon approach towards the seawall at 10 locations throughout Daytona Beach Shores. The distance between modeled surge extent, maximum surface water elevation along profile line, and maximum surge velocity along profile line are noted on each chart. Note the finer resolution of FLAVOR output and input as well as the greater surge extent modeled by FLAVOR.

XIV. CONCLUSIONS AND RECOMMENDATIONS

Model validation is made difficult due to the scarcity of observation data within the domain of refinement. The consistency between the performance of the previously validated HSOFS model and that of the FLAVOR model as demonstrated in the time series comparisons between model performance and NOAA Tides and Currents observations indicates that FLAVOR is a functioning model with predictive capabilities that are statistically comparable to those of HSOFS. FLAVOR results within the area of refinement cannot be regarded as superior on these grounds alone but may be regarded as computationally stable and scientifically reliable results. The presence of 3 validation sources within the domain of refinement and the statistically similar performance of FLAVOR and HSOFS (RMSE = 0.54 m, 0.48 m, respectively) conclude the integrity of FLAVOR results. It is not uncommon in engineering practice for a revised model to produce less accurate results than that which it is based upon in the first stage of refinement; this research therefore supports the continuation of development under the expectation that future FLAVOR results will be superior to those of HSOFS.

Metrics for velocity observations are non-existent in the domain of refinement; in fact, observation data for surge velocity is non-existent across the body of surge literature due to the difficulties associated with developing instrumentation for such metrics. The process of analyzing velocity therefore becomes a creative one, and velocity output of a validated model (such as HSOFS) is used as the sole source of comparison data. Discrepancies between the two models are primarily a result of increased resolution; in the case of FLAVOR modeled surge velocities reported as less than HSOFS modeled surge velocities along the coastline, this discrepancy is a direct result of the wetting/drying algorithm (i.e., FLAVOR resolution is finer than that of HSOFS, and therefore surge is allowed to propagate with reducing velocity up the slope of Volusia County's

coast where HSOFS models no velocity). Moreover, the spatial variability of Volusia County's coast, particularly within areas of steep elevation, gradient including seawalls and estuarine channels, is better represented in the FLAVOR model, hence the differences illustrated between peak velocity and elevation outputs of FLAVOR and HSOFS. These results are consistent with those anticipated from the onset of this thesis: increased resolution along a critical coastal feature (in the case of Volusia County, the seawalls which were destroyed in 2022, which represent vertical features of steep gradient) provides more detailed surge output that can be used as input parameters (i.e., applied force, soil saturation, etc.) for resilient seawall designs along Volusia County's coast.

The FLAVOR model, in its first iteration, is thereby complete, and the continuation of FLAVOR's development is highly recommended in order to produce scientific observations and predictions regarding the impact of storm surge on Volusia County's coast. Its careful development and implementation may eventually be used to investigate phenomena, such as the survival of New Smyrna Beach's seawalls throughout the 2022 hurricane season due to the 2004 city-wide upgrade of coastal armoring, as well as to inform policy and decision-making processes, such as the hazard mitigation plans implemented statewide in Florida that may be used to achieve countywide insurance discounts. Ultimately, FLAVOR's development is undertaken to fulfill the objective of contributing to a better-informed, environmentally adaptive Volusia County community.

XV. REFERENCES

- Abbott, Jim. (2023, November 9). 1 year after Tropical Storm Nicole, coastal residents in Daytona Beach area still struggle. *Daytona Beach News Journal*. [Hurricane Nicole: 1 year later, Florida coastal residents rebuilding \(news-journalonline.com\)](https://www.news-journalonline.com/story/news/2023/11/09/1-year-after-tropical-storm-nicole-coastal-residents-rebuilding/7000000001)
- Alizad, K., Hagen, S. C., Morris, J. T., Bacopoulos, P., Bilskie, M. V., Weishampel, J. F., & Medeiros, S. C. (2016). A coupled, two-dimensional hydrodynamic-marsh model with biological feedback. *Ecological Modelling*, 327, 29–43. doi:10.1016/j.ecolmodel.2016.01.013
- Bender, B., Knutson, K., Tuleya, T., Sirutis, S., Vecchi, V., Garner, G., & Held, H. (2010). Modeled impact of anthropogenic warming on the frequency of intense atlantic hurricanes. *Science*, 327(5964), 454–458. doi:10.1126/science.1180568
- Bilskie, M. V., Hagen, S. C., Alizad, K., Medeiros, S. C., Passeri, D. L., Needham, H. F., & Cox, A. (2016). Dynamic simulation and numerical analysis of hurricane storm surge under sea level rise with geomorphologic changes along the northern gulf of mexico. *Earth's Future*, 4(5), 177–193. doi:10.1002/2015EF000347
- Bilskie, M. V., Coggin, D., Hagen, S. C., & Medeiros, S. C. (2015). Terrain-driven unstructured mesh development through semi-automatic vertical feature extraction. *Advances in Water Resources*, 86, 102–118. doi:10.1016/j.advwatres.2015.09.020
- Catto, J. L., Shaffrey, L. C., & Hodges, K. I. (2011). Northern hemisphere extratropical cyclones in a warming climate in the HiGEM high-resolution climate model. *Journal of Climate*, 24(20), 5336–5352. doi:10.1175/2011JCLI4181.1

Childs, J. W. (2022). *Florida neighborhood struggles to recover from hurricane nicole*.

Retrieved from <https://www.wunderground.com/article/news/news/2022-12-05-florida-hurricane-nicole-wilbur-by-the-sea>

Coggin, David, “Lidar In Coastal Storm Surge Modeling: Modeling Linear Raised Features” (2008). *Electronic Theses and Dissertations*. 3478. <https://stars.library.ucf.edu/etd/3478>

Colle, B. A., Buonaiuto, F., Bowman, M. J., Wilson, R. E., Flood, R., Hunter, R., . . . Hill, D. (2008). New york city's vulnerability to coastal flooding: Storm surge modeling of past cyclones. *Bulletin of the American Meteorological Society*, 89(6), 829–842.
doi:10.1175/2007BAMS2401.1

Costanza, R., d'Arge, R., de Groot, R., Farber, S., Grasso, M., Hannon, B., . . . van den Belt, M. (1998). The value of the world's ecosystem services and natural capital. *Ecological Economics*, 25(1), 3–15. doi:10.1016/S0921-8009(98)00020-2

de Groot, A. V., Veeneklaas, R. M., & Bakker, J. P. (2011). Sand in the salt marsh: Contribution of high-energy conditions to salt-marsh accretion. *Marine Geology*, 282(3), 240–254.
doi:10.1016/j.margeo.2011.03.002

Dietrich, J. C., Tanaka, S., Westerink, J. J., Dawson, C. N., Luettich, R. A., Zijlema, M., Holthuijsen, L. H., Smith, J. M., Westerink, L. G., Westerink, H. J. (2012). Performance of the unstructured-mesh, SWAN+ADCIRC model in computing hurricane waves and surge. *Journal of Scientific Computing*, 52(2), 468–497. doi:10.1007/s10915-011-9555-6

Dietrich, J. C., Zijlema, M., Westerink, J. J., Holthuijsen, L. H., Dawson, C., Luettich, R. A., . . . Stone, G. W. (2010). Modeling hurricane waves and storm surge using integrally-coupled,

scalable computations. *Coastal Engineering*, 58(1), 45–65.

doi:10.1016/j.coastaleng.2010.08.001

Enwright, N. M., Griffith, K. T., & Osland, M. J. (2016). Barriers to and opportunities for landward migration of coastal wetlands with sea-level rise. *Frontiers in Ecology and the Environment*, 14(6), 307–316. doi:10.1002/fee.1282

Florida Department of Environmental Protection. (2022). *Hurricane Ian & Hurricane Nicole Post-Storm Beach Conditions and Coastal Impact Report*. Office of Resilience and Coastal Protection.

Fortunato, A., Bruneau, N., Azevedo, A., Araujo, M., & Oliveira, A. (2011). Automatic improvement of unstructured grids for coastal simulations. *Journal of Coastal Research*, 64, 1028–1032.

Funakoshi, Y., Hagen, S. C., & Bacopoulos, P. (2008). Coupling of hydrodynamic and wave models: Case study for hurricane floyd (1999) hindcast. *Journal of Waterway, Port, Coastal, and Ocean Engineering*, 134(6), 321–335. doi:10.1061/(ASCE)0733-950X(2008)134:6(321)

Helderop, E., & Grubestic, T. H. (2018). Hurricane Storm Surge in Volusia County, Florida: Evidence of a Tipping Point for Infrastructure Damage. *Disasters*, 43(1), 157–180. doi:10.1111/disa.12296

- Hu, R., Fang, F., Salinas, P., Pain, C. C., Sto.Domingo, N. D., & Mark, O. (2019). Numerical simulation of floods from multiple sources using an adaptive anisotropic unstructured mesh method. *Advances in Water Resources*, *123*, 173–188. doi:10.1016/j.advwatres.2018.11.011
- Lin, N., Emanuel, K., Oppenheimer, M., & Vanmarcke, E. (2012a). Physically based assessment of hurricane surge threat under climate change. *Nature Climate Change*, *2*(6), 462–467. doi:10.1038/nclimate1389
- Linhoss, A. C., Kiker, G., Shirley, M., & Frank, K. (2015). Sea-level rise, inundation, and marsh migration: Simulating impacts on developed lands and environmental systems. *Journal of Coastal Research*, *31*(1), 36–46. doi:10.2112/JCOASTRES-D-13-00215.1
- Luetlich, R. A., Westerink, J. J., & Scheffner, N. W. (1993). *ADCIRC: An advanced three-dimensional circulation model for shelves, coasts, and estuaries*.
- Marsooli, R., & Lin, N. (2018). Numerical modeling of historical storm tides and waves and their interactions along the U.S. east and gulf coasts. *Journal of Geophysical Research: Oceans*, *123*(5), 3844–3874. doi:10.1029/2017JC013434
- Medeiros, S. C., Bobinsky, J. S., & Abdelwahab, K. (2022). Locality of topographic ground truth data for salt marsh lidar DEM elevation bias mitigation. *IEEE Journal of Selected Topics in Applied Earth Observations and Remote Sensing*, *15*, 5766–5775. doi:10.1109/JSTARS.2022.3189226
- Medeiros, S. C., & Hagen, S. C. (2013). Review of wetting and drying algorithms for numerical tidal flow models. *International Journal for Numerical Methods in Fluids*, *71*(4), 473–487. doi:10.1002/flid.3668

National Oceanic and Atmospheric Administration. Retrieved from <https://www.noaa.gov/>. US Department of Commerce.

Riverside Technology Inc., & AECOM. (2015). Mesh development, tidal validation, and hindcast skill assessment of an ADCIRC model for the hurricane storm surge operational forecast system on the US Gulf-Atlantic coast.

Short, A. D. (1991). Macro-meso tidal beach morphodynamics: An overview. *Journal of Coastal Research*, 7(2), 417–436. Retrieved from <http://www.jstor.org/stable/4297847>

Szpilka, C., Dresback, K., Kolar, R., Feyen, J., & Wang, J. (2016). Improvements for the western north atlantic, Caribbean and Gulf of Mexico ADCIRC tidal database (EC2015). *Journal of Marine Science and Engineering*, 4(4) doi:10.3390/jmse4040072

Takahashi, H., Zdravković, L., Tsiampousi, A., & Mori, N. (2022). Destabilization of seawall ground by ocean waves. *Géotechnique*, , 1–16. doi:10.1680/jgeot.21.00420

Thomas, A., Dietrich, J. C., Dawson, C. N., & Luetlich, R. A. (2022). Effects of model resolution and coverage on storm-driven coastal flooding predictions. *Journal of Waterway, Port, Coastal, and Ocean Engineering*, 148(1) doi:10.1061/(ASCE)WW.1943-5460.0000687

The University of North Carolina at Chapel Hill. ADCIRC. <https://adcirc.org/>

Xian, S., Lin, N., & Hatzikyriakou, A. (2015). Storm surge damage to residential areas: A quantitative analysis for hurricane sandy in comparison with FEMA flood map. *Natural Hazards*, 79(3), 1867–1888. doi:10.1007/s11069-015-1937-x

Zaccarelli, N., Petrosillo, I., & Zurlini, G. (2008). Retrospective analysis. In S. E. Jørgensen, & B. D. Fath (Eds.), *Encyclopedia of ecology* (pp. 3020–3029). Oxford: Academic Press.
doi:10.1016/B978-008045405-4.00705-9 Retrieved
from <https://www.sciencedirect.com/science/article/pii/B9780080454054007059>

XVI. PUBLICATIONS

Medieros, S.C., Harbin, M. (2025), Refinement of a Regional Storm Surge Mesh for High

Resolution Topographic Representation of Volusia County, MDPI Water, Submission by

Dec. 31, 2024

Harbin, M. (2024, June 24-26) *Bolstering Local Resilience and Predictive Capability: building a*

research-grade surge model for Northeast Central Florida. (Poster) WaterSciCon24,

St. Paul, MN, USA.